



**INVESTIGATION ON PERFORMANCE OF DIFFERENT
STRUCTURAL MEMBERS REINFORCED WITH B600C-R REBAR AS
COMPARED TO B500CWR AND B420DWR REBAR**

Principal Investigator

Dr. Raquib Ahsan

Professor

Department of Civil Engineering, BUET



Department of Civil Engineering
Bangladesh University of Engineering and Technology

October 2022

ACKNOWLEDGEMENT

This research was conducted under the provision of the “Letter of Collaboration” signed between GPH Ispat and the Department of Civil Engineering, BUET on 3rd December 2018. I would like to express my gratitude to GPH Ispat. Without their material and financial support, it would be difficult to conduct the experiments. Research and Development Department of GPH Ispat extended their all-out cooperation while conducting research. I am truly thankful to their cooperation.

I would also like to extend my appreciation to the Department of Civil Engineering for accommodating space within the department for the purposes of this research. I would like to thank technical staff of the “Concrete & Materials Lab” and the “Strength of The Materials Lab” for their continuous support during the experiment.

ABSTRACT

With the advancement of technology and rapid increase in population, high rise buildings are becoming an important component of our life. For construction of high rise buildings, high strength materials are essential.

600 grade rebars are allowed by most of the standards and codes for building construction in different countries of the world. It is also specified in BDS ISO 6935-2. In our country, widely used rebar is B500CWR. Lower grade steels cause congestion in joints and reduce floor space. It is essential to determine the benefits and drawbacks of higher-grade steel (B600C-R) over conventional steel. In this research a comparative analysis has been performed to investigate the performance of different structural members reinforced with B420DWR, B500CWR and B600C-R. Column Interaction Diagram have been prepared for same column section by using different grades of steel.

Nine beams, nine columns and nine beam-column joints have been constructed to determine the performance of B600C-R rebar in different structural members. These specimens have been prepared by using different grades of steel (B420DWR, B500CWR, B600C-R) and concrete classes. The columns have been tested under compression load. Two-point flexure test has been conducted for the test of beams. The beam-column joints have been subjected to lateral cyclic loading test. Afterwards, the results have been analyzed to compare the performance of B600 C-R with B420DWR and B500CWR. Slabs, beams and columns have been designed using different grades of steel and reduction in steel consumption has been calculated. There is almost 30% saving in steel by using B600C-R when compared to B420DWR. Steel saving is 16% when B600C-R is compared to B500CWR. However, this reduction in steel consumption varies according to design.

The outcome of the experiment is that specimens reinforced with B600C-R show increase in load carrying capacity. From the results of beam-column joint test, it is evident that higher grade steel can sustain more lateral load and a greater number of cycles in push-pull cyclic load test. These results establish that B600 C-R can perform better especially for high rise buildings considering less congestions of steel and its beneficial impact on the environment.

TABLE OF CONTENTS

ACKNOWLEDGEMENT	i
ABSTRACT	ii
TABLE OF CONTENTS	iii
LIST OF TABLES	v
LIST OF FIGURES	vi
CHAPTER 1: INTRODUCTION	1
1.1 Background	1
1.2 Objectives of the Study	1
1.3 Methodology	2
1.4 Scope of the Investigation	4
1.5 Outline of the Study	4
CHAPTER 2: LITERATURE REVIEW	6
2.1 Introduction	6
2.2 Standards and Codes	6
2.3 High Strength Rebar Usage for Different Occupancies	9
2.4 Seismic Behavior of Joints with High Strength Steel Bars	11
2.5 Environmental Impact of Using Higher Grade Steel	11
2.6 Summary	11
CHAPTER 3: EXPERIMENTAL STUDY	12
3.1 Introduction	12
3.2 Material Properties	12
3.2.1 Cement	12
3.2.2 Fine Aggregate	13
3.2.3 Coarse Aggregate	14
3.2.4 Reinforcement	16
3.2.5 Concrete	16
3.3 Specimen Preparation	18
3.3.1 Reinforcement Preparation	18
3.3.2 Formwork Preparation	19
3.3.3 Mixing of Concrete	20

3.3.4	Concrete Casting	21
3.3.5	Curing of Specimen	21
3.3.6	White Coloring of Specimen	22
3.4	Experimental Study of Beam	22
3.4.1	Beam Test Results	23
3.4.2	Cracking Characteristics and Failure Patterns of Beam	24
3.4.3	Load vs Deflection Patterns of Beam	27
3.5	Experimental Study of Column	28
3.5.1	Column Test Results	29
3.5.2	Cracking Characteristics and Failure Patterns of Column	30
3.5.3	Load vs Deformation Patterns of Column	34
3.6	Experimental Study of Joint	35
3.6.1	Loading Protocol	37
3.6.2	Joint Test Results	37
3.6.3	Cracking Characteristics and Failure Patterns of Joint	38
3.6.4	Load- displacement Response of Joint	41
3.6.5	Stiffness Degradation	46
CHAPTER 4: DESIGN COMPARISONS		51
4.1	Beam Design Comparisons	51
4.2	Column Design Comparisons	53
4.2.1	Column Design of 8 Story Building	53
4.3	Slab Design Comparisons	55
4.4	Column Interaction Diagram	56
4.5	Comparison from Model	58
CHAPTER 5: CONCLUSIONS AND RECOMMENDATIONS		61
5.1	Introduction	61
5.2	Conclusions from the Experiments	61
5.3	Conclusions from the Design Comparisons	61
5.4	Conclusions from the Design of 10-Story Building	62
5.5	General Comments	62
5.6	Recommendations for Future Studies	63
REFERENCES		64

LIST OF TABLES

Table 1.1: Details of Specimen	2
Table 2.1: Steel Grades Specified in BDS ISO 6935-2: 2021	6
Table 2.2: Steel Grades Specified in ASTM 615-20	6
Table 2.3: Steel Grades Specified in ASTM 706-16	7
Table 2.4: Reinforcement Specified in ACI 318-19 for Different Structural Applications	7
Table 2.5: Rebar Strength in Design Codes for Various Countries	9
Table 3.1: Properties of Cement	12
Table 3.2: Properties of Fine Aggregate	13
Table 3.3: Properties of Coarse Aggregate	14
Table 3.4: Tension Test Results of Rebar	16
Table 3.5: Experimental Test Results of Beam	24
Table 3.6: Experimental Test Results of Column	30
Table 3.7: Axial Forces Applied on Column	37
Table 3.8: Experimental Test Results of Joints	38
Table 4.1: Steel Consumption Comparison in Beam for Different Grades of Steel	51
Table 4.2: Steel Consumption Comparison in Beam After Providing Rebar	52
Table 4.3: Steel Consumption Comparison in Column for Different Grades of Steel	53
Table 4.4: Steel Consumption Comparison in Column after Providing Rebar	54
Table 4.5: Steel Consumption Comparison in Slab for Different Grades of Steel	56
Table 4.6: Steel Consumption Comparison in Mat Foundation For Different Grades Of Steel	59
Table 4.7: Ground Floor Steel Consumption Comparison in Beam for Different Grades of Steel	60
Table 4.8: Ground floor Steel Consumption Comparison in Column for Different Grades of Steel	60

LIST OF FIGURES

Figure 1.1: Schematic diagram of beam specimen	3
Figure 1.2: Schematic diagram of column specimen	3
Figure 1.3: Schematic diagram of joint specimen	4
Figure 2.1: Comparison of rebar quantity according to the yield strength (after Cho and Lee, 2019)	10
Figure 2.2: Comparison of rebar quantity according to the yield strength for different structural elements of an underground parking (after Cho and Na, 2017)	10
Figure 3.1: Grain size distribution of sylhet sand	13
Figure 3.2: Grain size distribution of local sand.	14
Figure 3.3: Grain size distribution of 20 mm downgrade stone chips	15
Figure 3.4: Grain size distribution of 10 mm downgrade stone chips	15
Figure 3.5: Cylinder specimen casting and curing	16
Figure 3.6: Compressive strength test of concrete	17
Figure 3.7: Cylinder test result of 1 st phase specimen	17
Figure 3.8: Cylinder test result of 2 nd phase specimen	18
Figure 3.9: Cylinder test result of 3 rd phase specimen	18
Figure 3.10: Reinforcement preparation	19
Figure 3.11: Formwork preparation	20
Figure 3.12: Mixing of concrete	20
Figure 3.13: Casting of concrete	21
Figure 3.14: Curing of concrete	21
Figure 3.15: Specimen after white coloring	22
Figure 3.16: Schematic diagram of beam test setup	22
Figure 3.17: Two-point loading test setup of beam in laboratory	23
Figure 3.18: Cracks in beam reinforced with B420DWR and cast with 17.2 MPa concrete	24
Figure 3.19: Cracks in beam reinforced with B500CWR and cast with 17.2 MPa concrete	25
Figure 3.20: Cracks in beam reinforced with B600C-R and cast with 17.2 MPa concrete	25
Figure 3.21: Cracks in beam reinforced with B420DWR and cast with 24.1 MPa concrete	25
Figure 3.22: Cracks in beam reinforced with B500CWR and cast with 24.1 MPa concrete	25
Figure 3.23: Cracks in beam reinforced with B600C-R and cast with 24.1 MPa concrete	26

Figure 3.24: Cracks in beam reinforced with B420DWR and cast with 29.3 MPa concrete	26
Figure 3.25: Cracks in beam reinforced with B500CWR and cast with 29.3 MPa concrete	26
Figure 3.26: Cracks in beam reinforced with B600C-R and cast with 29.3 MPa concrete	26
Figure 3.27: Load vs deflection curves of beams for 17.2 MPa (2500 Psi) concrete	27
Figure 3.28: Load vs deflection curves of beams for 24.1 MPa (3500 psi) concrete	27
Figure 3.29: Load vs deflection curves of beams for 29.2 MPa (4250 psi) concrete	28
Figure 3.30: Schematic diagram of test setup of column	28
Figure 3.31 : Test set up of column for concentric axial load in laboratory	29
Figure 3.32: Failure patterns of column reinforced with (a) B420DWR (b) B500 CWR	31
Figure 3.33: Failure patterns of column reinforced with B600C-R	31
Figure 3.34: Failure patterns of column reinforced with (a) B420 DWR (b) B500 CWR	32
Figure 3.35: Failure patterns of column reinforced with B600C-R	32
Figure 3.36: Failure patterns of column reinforced with (a) B420DWR (b) B500 CWR	33
Figure 3.37: Failure patterns of column reinforced with (a) B420 DWR (b) B500 CWR	33
Figure 3.38: Load vs deformation curves of columns for 17.2 MPa concrete	34
Figure 3.39: Load vs deformation curves of columns for 24.1 MPa concrete.	34
Figure 3.40: Load vs deformation curves of columns for 29.3 MPa concrete	34
Figure 3.41: Schematic diagram of experimental setup of joint	36
Figure 3.42: Dial Gauge Positions of Joint Test	36
Figure 3.43: Loading protocol of joint test	37
Figure 3.44: Cracking characteristics of joint reinforced with B420DWR	39
Figure 3.45: Cracking characteristics of joint reinforced with B500CWR	39
Figure 3.46: Cracking characteristics of joint reinforced with B600C-R	40
Figure 3.47: Cracking characteristics of joint reinforced with (a) B420DWR (b) B500CWR	40
Figure 3.48: Cracking characteristics of joint reinforced with B600C-R	41
Figure 3.49: Load-Displacement response of joint reinforced with B420DWR and cast with 17.2 MPa concrete	41
Figure 3.50: Load-Displacement response of joint reinforced with B500CWR and cast with 17.2 MPa concrete	42
Figure 3.51: Load-Displacement response of joint reinforced with B600C-R and cast with 17.2 MPa concrete	42

Figure 3.52: Load-Displacement response of joint reinforced with B420DWR and cast with 24.1 MPa concrete	43
Figure 3.53: Load-Displacement response of joint reinforced with B500CWR and cast with 24.1 MPa concrete	43
Figure 3.54: Load-Displacement response of joint reinforced with B600C-R and cast with 24.1 MPa concrete	44
Figure 3.55: Load-Displacement response of joint reinforced with B420DWR and cast with 29.3 MPa concrete	44
Figure 3.56: Load-Displacement response of joint reinforced with B500CWR and cast with 29.3 MPa concrete	45
Figure 3.57: Load-Displacement response of joint reinforced with B600C-R and cast with 29.3 MPa concrete	45
Figure 3.58: Stiffness degradation curve of joint reinforced with B420DWR and cast with 17.2 MPa concrete	46
Figure 3.59: Stiffness degradation curve of joint reinforced with B500CWR and cast with 17.2 MPa concrete	46
Figure 3.60: Stiffness degradation curve of joint reinforced with B600C-R and cast with 17.2 MPa concrete	47
Figure 3.61: Stiffness degradation curve of joint reinforced with B420DWR and cast with 24.1 MPa concrete	47
Figure 3.62: Stiffness degradation curve of joint reinforced with B500CWR and cast with 24.1 MPa concrete	48
Figure 3.63: Stiffness degradation curve of joint reinforced with B600C-R and cast with 24.1 MPa concrete	48
Figure 3.64: Stiffness degradation curve of joint reinforced with B420DWR and cast with 29.3 MPa concrete	49
Figure 3.65: Stiffness degradation curve of joint reinforced with B500CWR and cast with 29.3 MPa concrete	49
Figure 3.66: Stiffness degradation curve of joint reinforced with B600C-R and cast with 29.3 MPa concrete	50
Figure 4.1: Bending moment diagram of beam	51
Figure 4.2: Selected column section for interaction diagram	56
Figure 4.3: Variation of column interaction diagram for B420DWR, B500CWR and B600C-R	57
Figure 4.4: 3D view of 10 story(G+9) residential Building	58
Figure 4.5: Plan view of 10 story(G+9) residential Building	59

CHAPTER 1

INTRODUCTION

1.1 Background

The economic activity of Bangladesh has taken a turnaround in recent times. Bangladesh has undertaken construction of many mega projects like the nuclear power plant, lengthy bridges, tunnels, high-rise buildings etc. However, for construction of structures with heavy loads, available lower grade reinforcing bars cause joint congestion and the resulting bigger structural sections eat up usable space. The situation becomes more challenging for seismic design of structures. With the increasing number of occurrences of earthquakes in Bangladesh, it has become essential to ensure the safety and sustainability of the reinforced concrete buildings against earthquakes (Siddique and Hossain, 2020). Prior to the 1970s, reinforced concrete buildings were only designed with gravity loads in mind, which resulted in very poor seismic performances. One of the main reasons behind the poor seismic performance of such old buildings is the weaknesses possessed by the beam-column joints (Pampanin et al., 2002; Kibria et al., 2020). Higher grade steel may address the congestion problem and may also provide enough floor space by reducing member size.

Higher grade can reduce the total amount of steel required for a construction and thereby reducing energy demand for production steel. Less amount of steel also implies less amount of exhaust gas and dust emissions during manufacturing process. Less amount of steel requirement will also reduce the construction efforts and time which can further reduce impacts of construction on environment.

Understanding the benefits and drawbacks of using higher grade steel is essential. Thus, the main purpose of this study is to investigate the behavior of higher grade steel in different structural elements, find out the optimum relation with different concrete classes, and determine the cost efficiency.

1.2 Objectives of the Study

The main objectives of this research are summarized below:

- i. To execute an experimental study on reinforced concrete structural elements i.e., beam, column and beam-column joints with 600-grade bars using different concrete classes.

- ii. To determine and compare compressive strength, bending moment, deflection, and serviceability for these elements.
- iii. To compare the results with members reinforced with lower grade steel.
- iv. To compare the seismic performance of beam-column joints cast with different steel grade and concrete class.
- v. To find out material savings & cost efficiency for using high-strength steel in beam, column & slab.

1.3 Methodology

The study is conducted in two steps. First experimental investigations are conducted to test structural performance of concrete members constructed with different grades of steel. Secondly, design comparisons are made of both individual concrete members and an integrated building.

The reinforced concrete members that will be investigated under the experimental study are beams, columns, and joints. At first, the beam will be designed for two point loading flexure strength test using different steel grades and concrete classes. The steel grades that will be used are B420DWR, B500CWR, and B600C-R. Concrete mix will be used to achieve compressive strength of 17.2 MPa (2500 psi), 24.1 MPa (3500 Psi) & 29.3 MPa (4250 Psi). Beam size will be full-scale (3000 x 300 x 250 mm) and column size will be half-scale (1500 x 200 x 200 mm). The joints will be full-scale. A total of 9 beams, 9 columns, and 9 joints will be cast. For beam, column and joint 16mm bar will be placed as main reinforcement and we will use 8 mm bar as the stirrup/tie bar. Then the specimens will be tested by following appropriate procedure. Finally, the data will be analyzed thoroughly. Details of specimen are shown in Table 1.1. Details of the test specimens are shown in Figures 1.1 to 1.3.

In the design comparison, designs of beams, columns and slabs were compared. Concrete sections of these elements were kept unchanged and steel quantities were only varied. The required quantity of steel was then compared. Finally, a 10-storied residential building was modelled and analyzed. Steel requirement for the ground floor and mat foundation was calculated separately for different grades of steel. The steel requirement for different grades of steel was then compared.

Table 1.1: Details of Specimen

Details of Specimen	Concrete Strength, MPa (Psi)	Steel Grade, MPa (Minimum yield stress, ksi)
Beam , Column and Beam-Column Joint	17.2 (2500)	B420DWR (60)
		B500CWR (72.5)
		B600C-R (87)
	24.1 (3500)	B420DWR (60)
		B500CWR (72.5)
		B600C-R (87)
	29.3 (4250)	B420DWR (60)
		B500CWR (72.5)
		B600C-R (87)

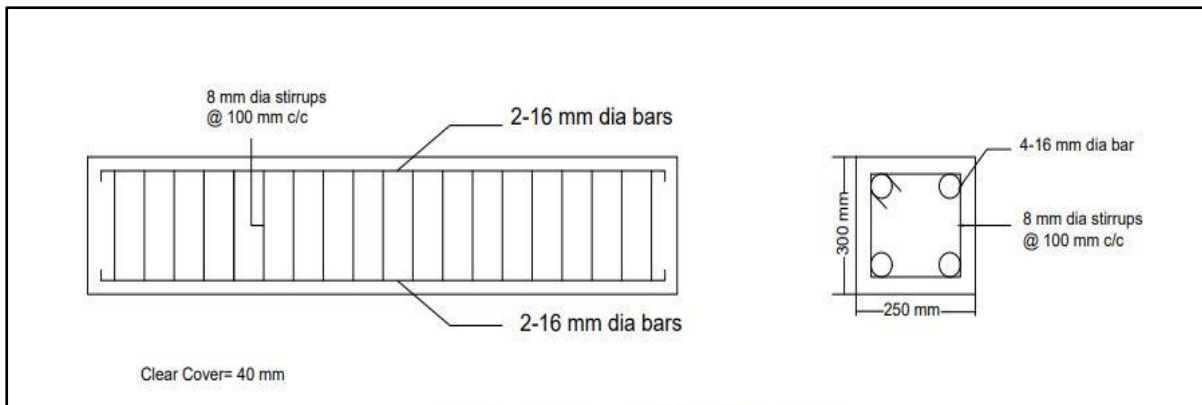


Figure 1.1: Schematic Diagram of Beam Specimen (3000X300X250 mm)

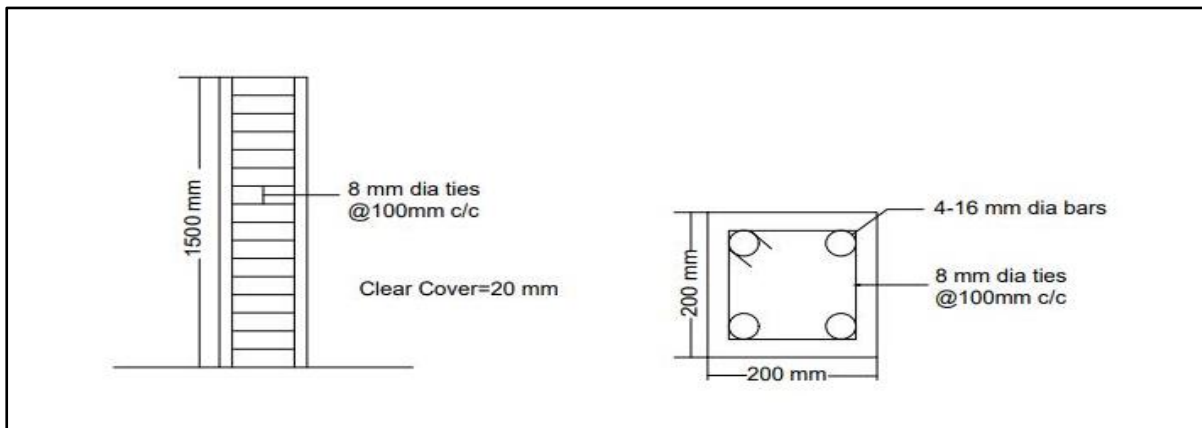


Figure 1.2: Schematic Diagram of Column Specimen (1500X200X200 mm)

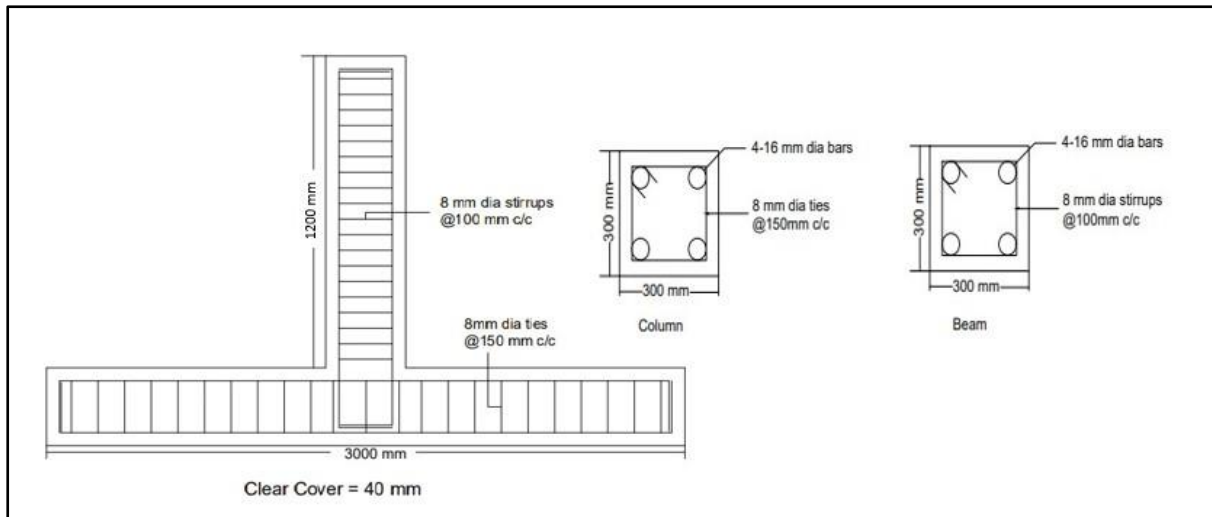


Figure 1.3: Schematic Diagram of Joint Specimen

1.4 Scope of the Investigation

The present study involves both experimental investigation of structural performance and design comparison of quantity saving of different grades of steel. The experimental study deals with a preliminary investigation of physical specimens of beam, column and beam-column joint reinforced with different grades of steel. Beam and joint specimens were prepared in full scale. The column specimens were prepared in half scale due to limitation of load capacity of the Universal Testing Machine (UTM) available in the laboratory at BUET. B420DWR, B500 CWR and B600C-R 16 mm bars have been used in this research. 8mm diameter B420DWR has been used for tie and stirrup. Both local sand and Sylhet sand have been used. The columns have been tested under compression load. Two-point flexure test has been conducted for the test of beams and the beam-column joints have been subjected to lateral cyclic loading test.

For design comparison a beam with a span length of 5m is designed for different steel grades and concrete classes. The section of the beam was chosen as 375X300 mm and the uniformly distributed load on beam is considered to 72kN/m. An interior column with span length of 5m on both sides is designed using different concrete classes and steel grades for comparison. 200 psf load is considered on the column tributary area. For comparison of design of slabs, a two way slab supported on all four edges is designed for different steel grades.

1.5 Outline of the Study

To appropriately present the topic in a sequential manner, this research has been divided into five chapters.

Chapter One includes background of the research, methodology, objectives and outline of the study.

Chapter Two contains 'Literature Review' which describes the past research about higher grade steel and their findings.

Chapter Three includes material properties, specimen preparation, test setup and results from the experiment.

Chapter Four presents the savings of steel consumption for using higher grade steel.

Chapter Five summarizes the experiment's general finding and offers recommendations for further research.

CHAPTER 2

LITERATURE REVIEW

2.1 Introduction

It is obvious for the high-rise and long span structure, using of excessive rebars causes congestion and finally lowers the quality of the structure. Due to the lack of high strength steel rebar, engineers are bound to use lower grade steel in a huge quantity. The use of higher strength steel like B600C-R can be an impactful solution to this problem along with the improvement of the constructability, reduction of cross-sectional area and construction period and relieve of joint congestion by simplifying detailing. Previous research works mainly focused on minimizing the work processing loss, improving the rebar work method, and studying for the improvement of the rebar work. This research is carried out to find out the reduction ratio as well as applicability of the high strength reinforcing bar.

2.2 Standards and Codes

BDS ISO 6935-2:2021 specifies chemical composition and mechanical properties of higher steel grades like 600 and 700 in its latest version as it has adopted the latest ISO standards for ribbed bars (Table 2.1).

Table 2.1: Steel Grades Specified in BDS ISO 6935-2: 2021

Steel Grade	Minimum Upper Yield Strength, R_{eH} MPa	Ductility Class	Tensile and Yield Strength Ratio R_m/R_{eH}
B500C-R	500	C	1.15
B600C-R	600		
B700C-R	700		
B420DWR	420	D	1.25
B500D-R	500		
B600D-R	600		
B700D-R	700		

ASTM standard A615-20 specifies higher grade steel like Grade 80 [550] and Grade 100 [690] (Table 2.2). A706-16 standard which is particularly for steel with enhanced weldability specifies grade 80 [550] (Table 2.3).

Table 2.2: Steel Grades Specified in ASTM 615-20

Steel Grade	Minimum Yield Strength, MPa	Tensile and Yield Strength Ratio
60	420	1.10
80	550	
100	690	

Table 2.3: Steel Grades Specified in ASTM 706-16

Steel Grade	Minimum Yield Strength, MPa	Maximum Yield Strength, MPa
60	420	540
80	550	675

ACI 318-19 allows use of steel with yield strength (f_y) exceeding 80,000 psi for slab design.¹ For beams² and columns,³ ACI 318-19 allows use of steel with $f_y \geq 80,000$ psi as longitudinal reinforcement with special requirements for transverse reinforcement along development and lap splice lengths. According to ACI 318-19, ASTM A706 Grades 80 and 100 reinforcements, except bar sizes larger than No. 18 (57.3 mm), are permitted to resist moments, axial, and shear forces in special structural walls and all components of special structural walls, including coupling beams and wall piers.⁴ ASTM A706 Grade 80 reinforcement, except bar sizes larger than No. 18 (57.3 mm), is also permitted in special moment frames.⁵ The use of Grade 100 reinforcement is, however, not allowed in special moment frames. Types of reinforcements that are specified by ACI 318-19 for particular structural applications are given in Table 2.4.

Table 2.4: Reinforcement Specified in ACI 318-19 for Different Structural Applications

Usage	Application		Maximum value of f_y permitted for design calculations, psi
Flexure; axial force; and shrinkage and temperature	Special seismic systems	Special moment frames	80,000
		Special structural walls	100,000
	Other		100,000
Lateral support of longitudinal bars; or Concrete confinement	Special seismic systems		100,000
	Spirals		100,000
	Other		80,000
Shear	Special seismic system	Special moment frames	80,000
		Special structural walls	100,000
	Spirals		60,000
	Shear friction		60,000
	Stirrups, ties, hoops		60,000
Torsion	Longitudinal and transverse		60,000
Anchor reinforcement	Special seismic systems and other		80,000
Regions designed using strut-and-tie method	Longitudinal ties		80,000
	Other		60,000

¹ Section 8.3.1.1 and Table 8.3.1.1 of ACI 318-19, Page 101.

² Section 9.7.1.4 of ACI 318-19, Page 139.

³ Section 10.7.1.3 of ACI 318-19, Page 159.

⁴ Section R18.2.6.1 of ACI 318-19, Page 289.

⁵ Section R18.2.6.1 of ACI 318-19, Page 289.

To allow the use of ASTM A706 Grade 80 and 100 reinforcement, ACI 318-19 Code includes limits for spacing of transverse reinforcement to provide adequate longitudinal bar support to control longitudinal bar buckling. In special moment frames, the use of Grade 80 reinforcement requires increased joint depths to prevent excessive slip of beam bars passing through beam-column joints.

According to Bangladesh National Building Code (BNBC) 2020,⁶ deformed reinforcing bars shall conform to the following Standards; BDS ISO 6935-2:2010, Steel for the reinforcement of concrete - Part-2: Ribbed bars; Reinforcement conforming to the ASTM, Standards: A615/A615M Deformed and Plain Billet-Steel Bars; A616M, Rail-Steel Deformed and Plain Bars; A617M Axle-Steel Deformed and Plain Bars; A706M Low-Alloy Steel Deformed Bars; A767M Zinc Coated (Galvanized) Steel Bars; and A775M Epoxy-Coated Reinforcing Steel. Deformed reinforcing bars with a specified yield strength f_y exceeding 410 MPa may be used, provided f_y shall be the stress corresponding to a strain of 0.35 percent and the bars otherwise conform to ASTM standards noted above.

However, for reinforcement in special moment frames and special structural walls, deformed reinforcement resisting earthquake-induced flexural and axial force, or both, shall comply with ASTM A706 Grade 420.⁷ Alternatively, only BDS ISO 6935-2 Grades 300, 350, 400 and 420 or ASTM A615 Grades 275 and 420 reinforcements shall be with some restrictions including that the ratio of the actual tensile strength to the actual yield strength is not less than 1.25.

On the other hand, BNBC 2020 does not prevent the use of any new and alternative materials.⁸ Any such material may be approved provided it is shown to be satisfactory for the purpose intended and at least equivalent of that required in quality, strength, effectiveness, fire resistivity, durability, safety, maintenance and compatibility.

In many countries in different parts of the world high strength rebars are allowed for different types of structural applications. Table 2.5 summarizes use of high strength rebars in different countries. The table shows that in most of the countries 600 grade steel is allowed for building structures.

⁶ Section 2.3.6 of Chapter 2, Part 5, BNBC 2020.

⁷ Section 8.3.3.4 of Chapter 8, Part 6, BNBC 2020.

⁸ Section 2.1.1 of Chapter 2, Part 5, BNBC 2020.

Table 2.5: Rebar Strength in Design Codes for Various Countries

Code	KCI, 2012	EUROCODE 2	BCA	BDS, 2012	AASHTO, 2017
Structure	Building	Building and Bridge		Bridge	
Country	Korea	EU	Singapore	Korea	USA
Reinforcement (Flexural Member), MPa	600	600	600	600	690
Reinforcement (Flexural & Axial Member), MPa	600	600	600	500	560

2.3 High Strength Rebar Usage for Different Occupancies

Cho and Lee (2019) investigated the reduction ratio and applicability of the high strength reinforcing bars (SD500, SD600) to three types of structural systems (rahmen structure, bearing wall system and flat plate system) for buildings in Korea. In this study they found that the reduction ratio of the high strength bars on the horizontal members was higher than the vertical members in general. Among the horizontal members, beam and foundation showed a similar decrease in each structure. On the other hand, in case of slabs, the reduction ratio of the re-bar was large according to the type of the structure. For the mixed-used residential complex building the decreasing ratio of the re-bar was significant when slabs strengths were large. But, in the case of apartment buildings re-bar ratio decreasing was highly governed by the minimum requirement and the spacing of the re-bar, while the amount of the rebar was rather increased due to the restriction of crack spacing in the case of office buildings (Figure 2.1).

In general, it was found that the use of high strength reinforcing bars reduces the amount of reinforcement work and shortens the construction period due to the reduced reinforcing bars. Finally, they concluded that the economizing effect is greater if considering the qualitative effects such as the improvement of the workability and the quality improvement of the structure due to the proper spacing of the re-bars.

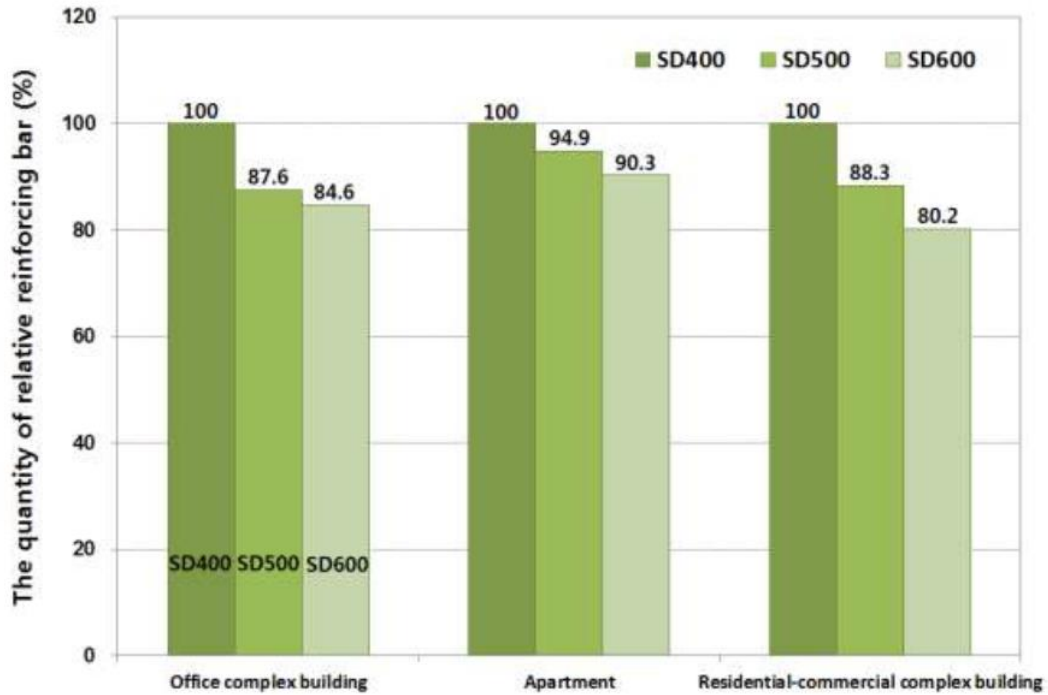


Figure 2.1: Comparison of rebar quantity according to the yield strength (after Cho and Lee, 2019)

Cho and Na (2017) investigated quantity variations of the high-strength reinforcing bars on the underground parking spaces in a rigid-structure building. They showed that the total quantity of reinforcement was reduced 11.1 per cent on SD500 rebars comparing with SD400 (Figure 2.2). It would be possible to lower the amount of reinforcing bars up to 20.6 per cent, when SD600 rebars were used comparing with SD400 ones.

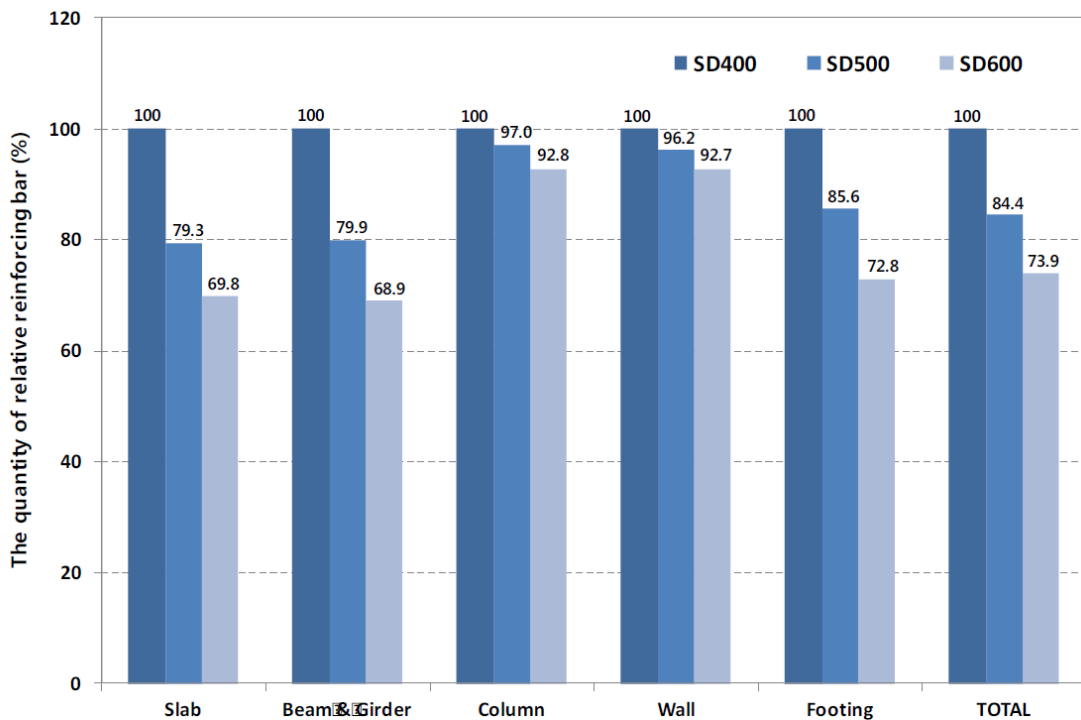


Figure 2.2: Comparison of rebar quantity according to the yield strength for different structural elements of an underground parking (after Cho and Na, 2017)

2.4 Seismic Behavior of Joints with High Strength Steel Bars

Feng et al. (2020) conducted an experimental investigation of the seismic performance of interior beam–column joints with beams reinforced with Grade 600MPa longitudinal steel bars. Comparisons performed between specimens demonstrate that among the beam–column joints with 600 MPa high strength steel bars, specimens with high reinforcement ratios have better energy dissipation capacity, slower stiffness degradation, and lower ductility.

2.5 Environmental Impact of Using Higher Grade Steel

Yao et al. (2020) presented an estimate that saving of 10 million tons of steel is equivalent to saving 18 million tons of iron ore which in turn saves 6.5 million tons of standard coal reducing requirements of significant amount of exhaust gas and dust emissions. From these statistics, the authors inferred that application of high-strength rebar can save energy and resources as well as harmful emissions.

2.6 Summary

The literature review conducted in this study amply showed that 600 grade rebars are allowed by most of the standards and codes for building construction in different countries of the world. It is also specified in BDS ISO 6935-2. BNBC 2020 followed an older version of ACI 318, namely ACI 318-08, where restriction was imposed on the use of grades higher than 420 MPa for special moment frames and special structural walls. However, ACI 318-19 does not impose such restriction. Moreover, BNBC 2020 states that it does not prevent the use of any new material if it is shown to be satisfactory in quality, strength, stiffness etc. Thus, legally there should not be any obstruction in using 600 grade steel in building construction in Bangladesh if its performance can be shown to be satisfactory for the purpose it is used.

Literature also shows that considerable saving in material quantities can be achieved by using 600 grade rebar as compared to 500 grade or 400 grade rebars. The necessity of lesser rebar size also results in reduced development and splice length. The most important advantage of using higher grade steel is less congestion in concrete resulting in better concrete quality. Moreover, less requirement of steel ultimately has a positive impact on environment. Now, it is required to investigate how much saving can be possible using 600 grade steel while designing structures according to BNBC 2020.

CHAPTER 3

EXPERIMENTAL STUDY

3.1 Introduction

An experimental study is necessary to ascertain the behavior of structural members reinforced with higher grade steel. This chapter covers the characteristics of the materials used in the research, the specifics of the model that was chosen, the description and method of specimen preparation, the experimental setup and instruments, as well as the method of data collection.

3.2 Material Properties

Cement, fine aggregate, coarse aggregate, and steel reinforcement are main components of reinforced concrete. Sylhet sand and locally available sand have been used as fine aggregate. 20 mm downgrade stone chips have been used for beam and joint casting, while 10 mm downgrade stone chips have been used for column casting. All these materials have been tested in the laboratory to ensure proper quality. Compressive strength of concrete was also obtained by conducting compression test of cylinder specimen in the laboratory.

3.2.1 Cement

Crown Portland Cement (BDS EN 197-1:2003) has been used in this research. Some essential properties of this cement have been determined in the concrete laboratory.

The properties are shown in Table 3.1.

Table 3.1: Properties of cement

Normal Consistency (%)	25
Initial setting time (minutes)	162
Final setting time (minutes)	358
Cement mortar compressive strength	
7 days (MPa)	35.4
28 days (MPa)	46.2

3.2.2 Fine Aggregate

Sylhet sand and locally available sand have been used as fine aggregate. According to ASTM C128-01, the specific gravity and water absorption of sand have been measured in a laboratory. The sieve analysis was performed in accordance with ASTM C136. The properties of the fine aggregates are shown in Table 3.2.

Table 3.2: Properties of Fine Aggregate

Properties	Sylhet Sand	Local Sand
Specific Gravity	2.72	2.64
Water Absorption Capacity	0.91%	0.94%
Fineness Modulus	3.36	1.11

Grain size distribution curve for Sylhet sand is shown in Figure 3.1 and grain size distribution curve for local sand is shown in Figure 3.2.

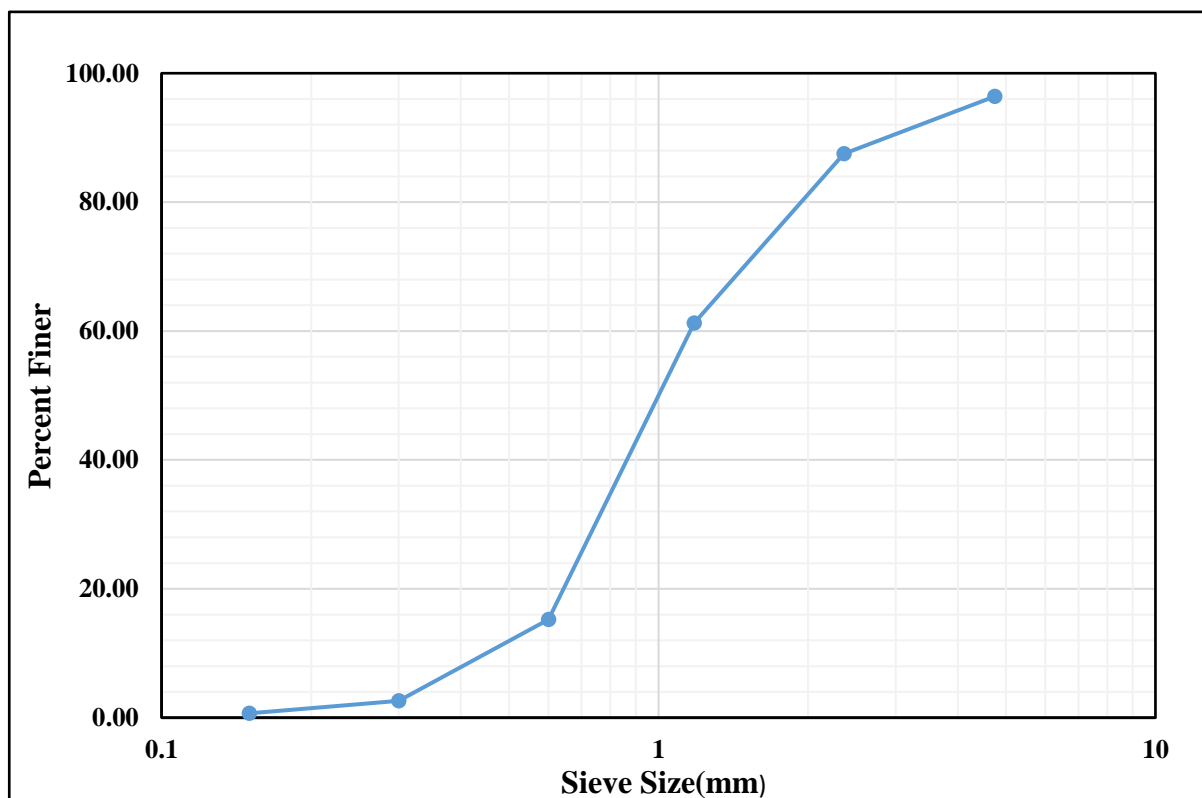


Figure 3.1: Grain Size Distribution of Sylhet Sand

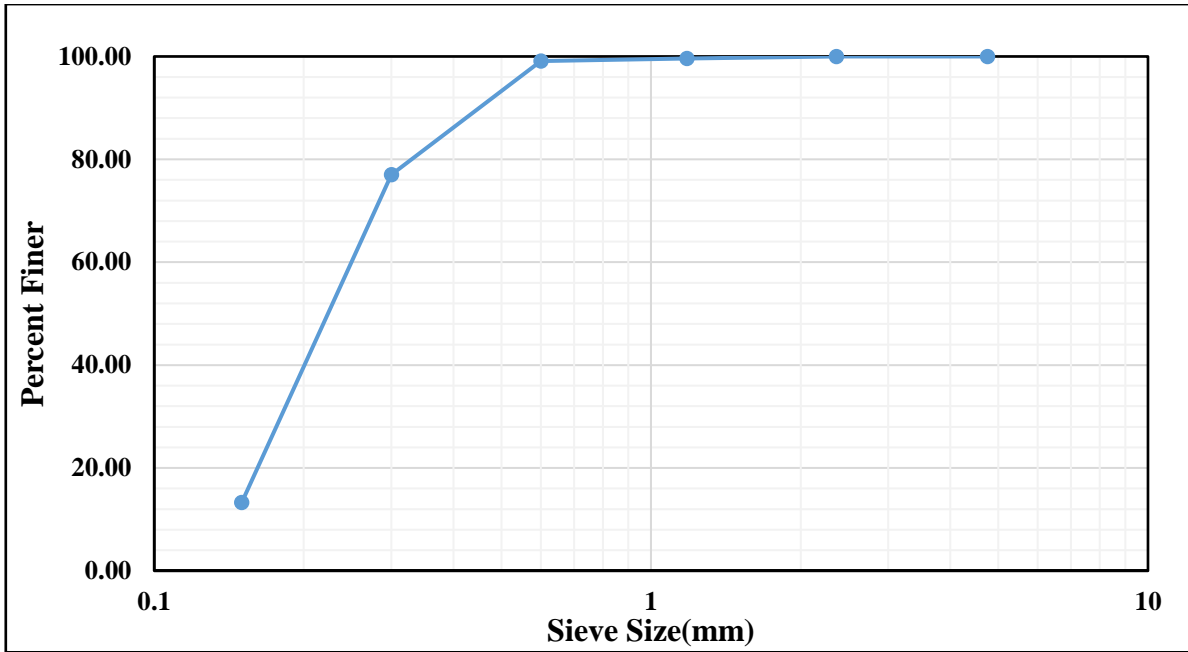


Figure 3.2: Grain Size Distribution of Local Sand.

3.2.3 Coarse Aggregate

20 mm downgrade stone chips and 10 mm downgrade stone chips were used in this research. Specific gravity and water absorption of coarse aggregates have been determined in accordance with ASTM C127. Sieve analysis was performed in accordance with ASTM C136. Properties of coarse aggregates are shown in Table 3.3.

Table 3.3: Properties of coarse aggregate

Parameter	20 mm downgrade stone chips	10 mm downgrade stone chips
Bulk Specific Gravity	2.67	2.65
Water Absorption Capacity	0.75%	0.82%
Fineness Modulus	6.72	4.84

Grain Size distribution curve of 20 mm downgrade stone chips is shown in Figure 3.3. Grain size distribution curve of 10 mm downgrade stone chips is shown in Figure 3.4.

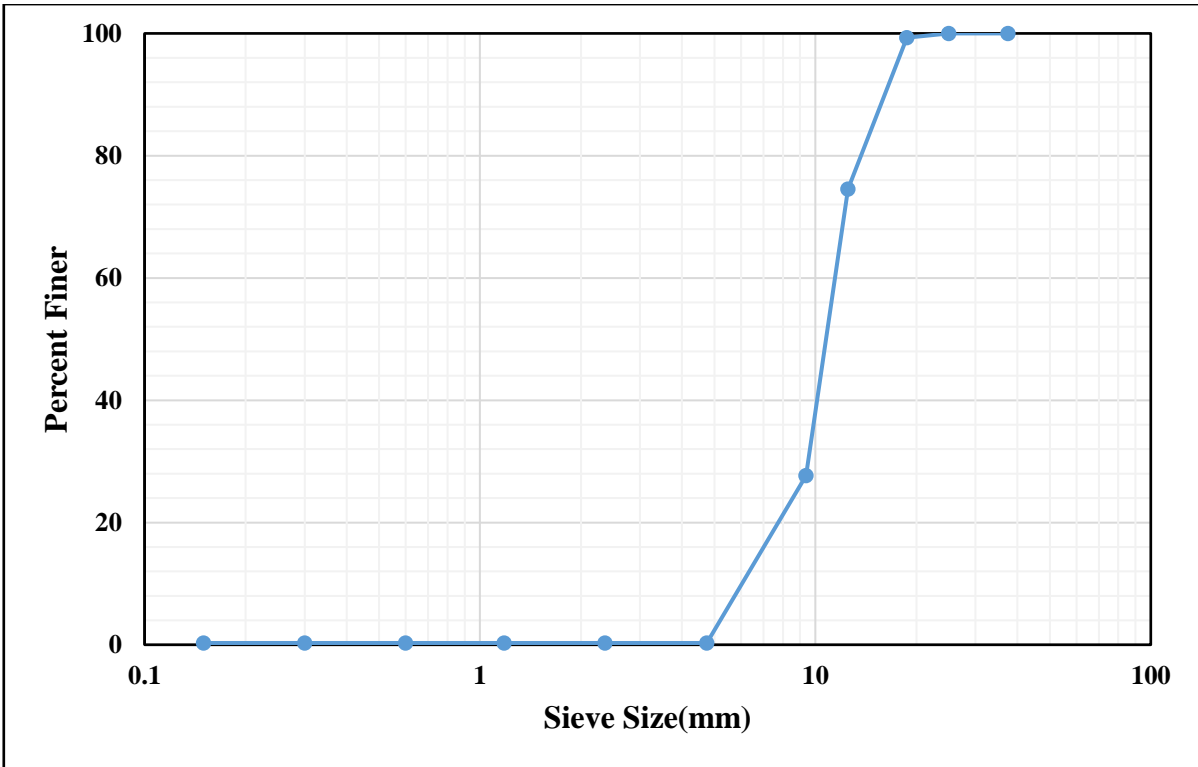


Figure 3.3: Grain Size Distribution of 20 mm downgrade stone chips

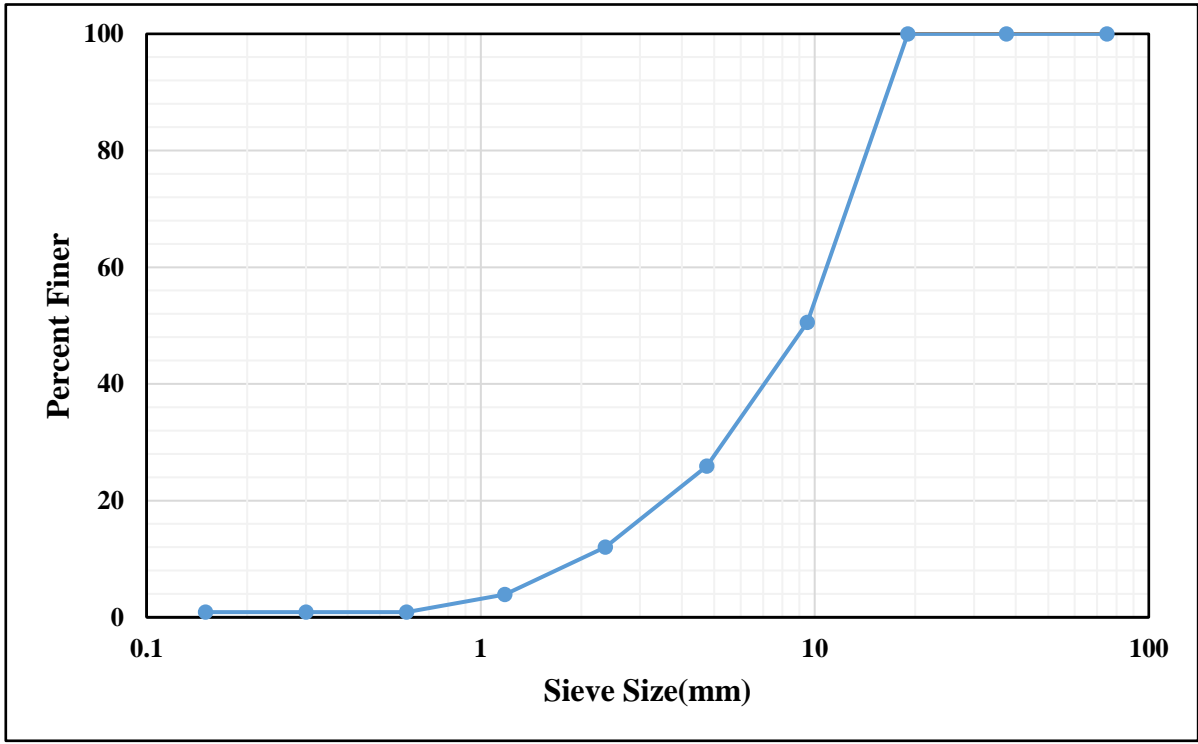


Figure 3.4: Grain Size Distribution of 10 mm downgrade stone chips

3.2.4 Reinforcement

Reinforcements of three grades (420MPa, 500 MPa, 600 MPa) have been used in this research work. For transverse reinforcements 8 mm rebar (420 MPa) have been used. Tension test results are shown in Table 3.4.

Table 3.4: Tension test results of rebar.

Rebar Grade	Diameter (mm)	Weight (kg/m)	Cross-Sectional Area (mm ²)	Yield Load (N)	Ultimate Load (N)	Ultimate Load/Yield Load	Yield Strength (MPa)	Elongation (%)
B600C-R	16	1.57	201	129030	149987	1.16	642	14
B500CWR	16	1.55	201	113040	132631	1.17	562	15
B420DWR	16	1.57	201	94077	130767	1.39	468	17
B420DWR	8	0.41	50	23348	32990	1.41	467	15

3.2.5 Concrete

Three different classes of concrete were prepared using variable proportions of cement, sand and stone chips. 20 mm downgrade stone chips have been used for beam and joint casting, while 10 mm downgrade stone chips have been used for column casting. Slump value 75-100 mm were achieved to ensure sufficient workability. The compressive strengths of concrete have been determined by performing compression tests in accordance with ASTM C39. The concrete cylinders were cured for 28 days. After curing period, these cylinders were tested in compression testing machine.



Figure 3.5: Cylinder Specimen Casting and Curing



Figure 3.6: Compressive Strength test of Cylinder

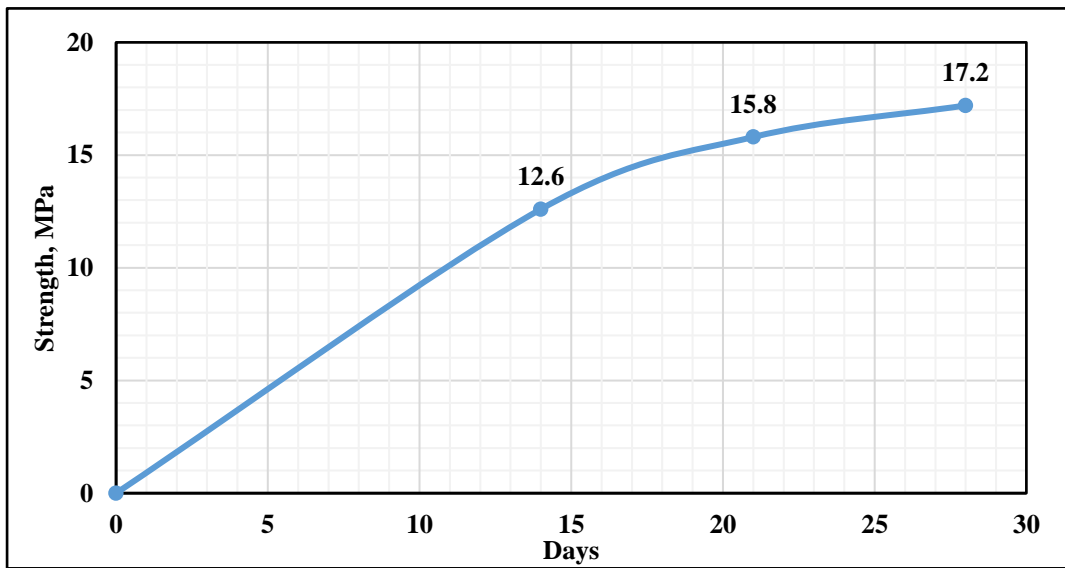


Figure 3.7: Cylinder test result of 1st phase specimen

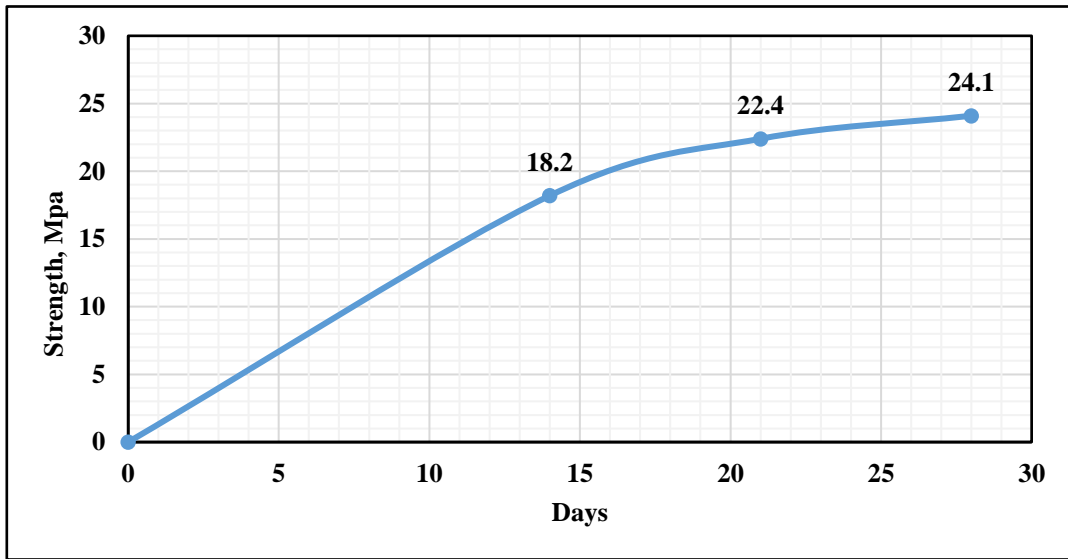


Figure 3.8: Cylinder test result of 2nd phase specimen

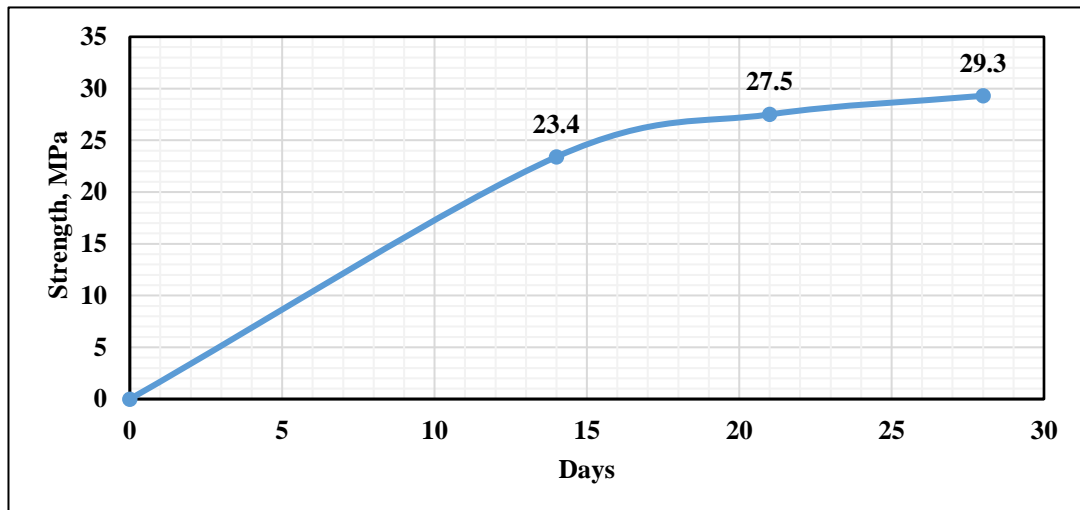


Figure 3.9: Cylinder test result of 3rd phase specimen

3.3 Specimen Preparation

The test samples have been prepared in the laboratory. With the help of experienced laboratory staff, quality of the samples have been assured.

3.3.1 Reinforcement Preparation

According to the details of the specimens shown in Figures 1.1 to 1.3, reinforcements were bound. It was made sure that there was adequate clear cover, and the reinforcements were positioned correctly. In accordance with the requirements of BNBC 2020, the ties and stirrups were appropriately hooked at the ends. For joint specimens, the ties have been maintained

throughout the joint region. After being prepared, the reinforcements were inserted inside the formworks, which provided suitable clear cover using cement concrete blocks.

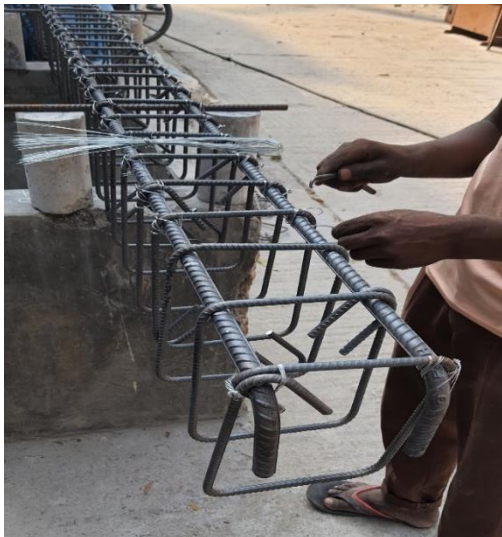


Figure 3.10: Reinforcement Preparation

3.3.2 Formwork Preparation

To manage the shape and give the freshly flowing concrete stability, formwork is needed. The formwork must endure any and all loads imposed by materials, equipment, workers, or environmental loads in addition to the weight and pressure of the concrete during casting. Until the concrete sets and hardens and becomes strong enough to support itself and applied loads, formwork supports the structure. Timber formworks have been used in this study. The joints of the formworks have been checked to make sure they do not leak.



Figure 3.11: Formwork Preparation

3.3.3 Mixing of Concrete

By altering proportions of particles in each mix, different concrete mixtures have been achieved. The motorized mixing machine was filled with the proper amounts of cement, sand, coarse aggregate, and water to ensure that the concrete was thoroughly and uniformly mixed. Slump has been measured to ensure that concrete is sufficiently workable. Slump value was between 75-100 mm.



Figure 3.12: Mixing of Concrete

3.3.4 Concrete Casting

Fresh concrete mix was carefully poured on the formwork. Clear cover was maintained using concrete blocks. Compaction of concrete was done using mechanical vibrator to ensure that no air void exists in concrete.



Figure 3.13: Casting of Concrete

3.3.5 Curing of Specimen

To gain required strength of concrete, curing is very important. Curing started after final setting time of concrete.



Figure 3.14: Curing of Specimen

3.3.6 White Coloring of Specimen

After 28 days of curing, formworks were removed. Specimens have been colored with white paint for better visibility of cracks.



Figure 3.15: Specimen after white coloring.

3.4 Experimental Study of Beam

Beam specimens were tested under two point loading with 900 mm span on either side of the loading points. Total support to support span length of the test beam was 2700 mm. Load was applied in two points at 900 mm distance at the middle of the beam. A universal testing machine (UTM) with a loading capacity of 1500 kN has been used for the test. Data was collected using three dial gauges at the bottom of the beam. Schematic Diagram of beam test setup is shown in Figure 3.16.

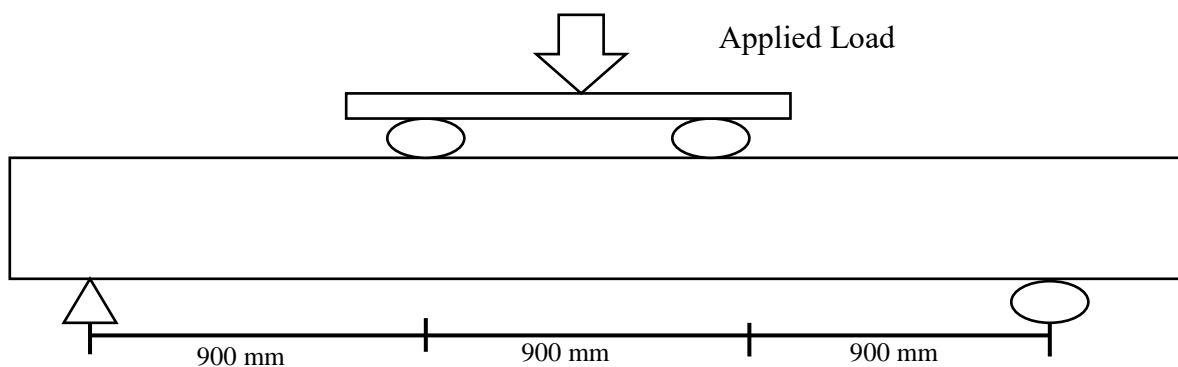


Figure 3.16: Schematic Diagram of Beam Test Setup

The beams were placed in the UTM according to the test plan. Two circular steel bars were used to distribute the load in two points. There was enough gap between the machine and the load spreader beam. A constant load rate of 15 kN/min was employed for these beams throughout the loading process.



Figure 3.17: Two-point loading test setup of beam in laboratory

3.4.1 Beam Test Results

Beam is a flexural member. When load is applied to beam, bottom portion experiences tension and top portion compression. Beams are always designed as under-reinforced members. So that, steel yields before concrete crushes. Moment capacity of beam chiefly governs by steel. However concrete strength also influences flexural capacity of beam. From Table 3.5, it is visible that, moment capacity of the beam increases when beam is reinforced with higher grade steel. However, Moment capacity of beam increases significantly with the increase in concrete strength. Higher grade concrete reduces the depth of compression block which eventually increases the moment arm. As a result, moment capacity of beam increases with higher grade steel and concrete.

Table 3.5: Experimental test results of beam.

Beam Dimension, mm	Concrete Strength, MPa(Psi)	Steel Grade, MPa	Design Moment Capacity, kN-m	Experimental Moment Capacity, kN-m	Remarks
300X250	17.2 (2500)	420	35.97	49.5	Satisfactory
		500	42.01	53.55	Satisfactory
		600	49.21	54.9	Satisfactory
	24.1 (3500)	420	37.00	51.75	Satisfactory
		500	43.48	56.7	Satisfactory
		600	51.32	58.95	Satisfactory
	29.3 (4250)	420	37.44	52.2	Satisfactory
		500	44.10	57.6	Satisfactory
		600	52.21	60.3	Satisfactory

3.4.2 Cracking Characteristics and Failure Pattern of Beam

As two point loading was applied, maximum bending moment was generated at middle portion of the beam. Cracks become visible when 30-35% of the ultimate load was applied. The beam specimens failed due to flexure. Cracking characteristics of the specimen are shown from figure 3.18 to 3.26.



Figure 3.18: Cracks in beam reinforced with B420DWR and cast with 17.2 MPa concrete



Figure 3.19: Cracks in beam reinforced with B500CWR and cast with 17.2 MPa concrete



Figure 3.20: Cracks in beam reinforced with B600C-R and cast with 17.2 MPa concrete



Figure 3.21: Cracks in beam reinforced with B420DWR and cast with 24.1 MPa concrete



Figure 3.22: Cracks in beam reinforced with B500CWR and cast with 24.1 MPa concrete



Figure 3.23: Cracks in beam reinforced with B600C-R and cast with 24.1 MPa concrete



Figure 3.24: Cracks in beam reinforced with B420DWR and cast with 29.3 MPa concrete



Figure 3.25: Cracks in beam reinforced with B500CWR and cast with 29.3 MPa concrete



Figure 3.26: Cracks in beam reinforced with B600C-R and cast with 29.3 MPa concrete

In low strength concrete crack starts to appear early compared to high strength concrete. For beams reinforced with B420 DWR deflection is much higher than beams reinforced with B500 CWR and B600C-R. Higher deflection occurs due to the difference in ductility class.

3.4.3 Load vs Deflection Patterns of Beam

Load vs deflection graphs of beams reinforced with B420DWR, B500CWR and B600C-R for concrete classes of 17.2, 24.1 and 29.3 MPa are shown in Figures 3.27 to 3.29. These graphs signify that beams reinforced with B600C-R can sustain more load than beam reinforced with B420 DWR and B500CWR. Eventually, Moment capacity of beams reinforced with B600C-R is higher than beams reinforced with B420DWR and B500CWR.

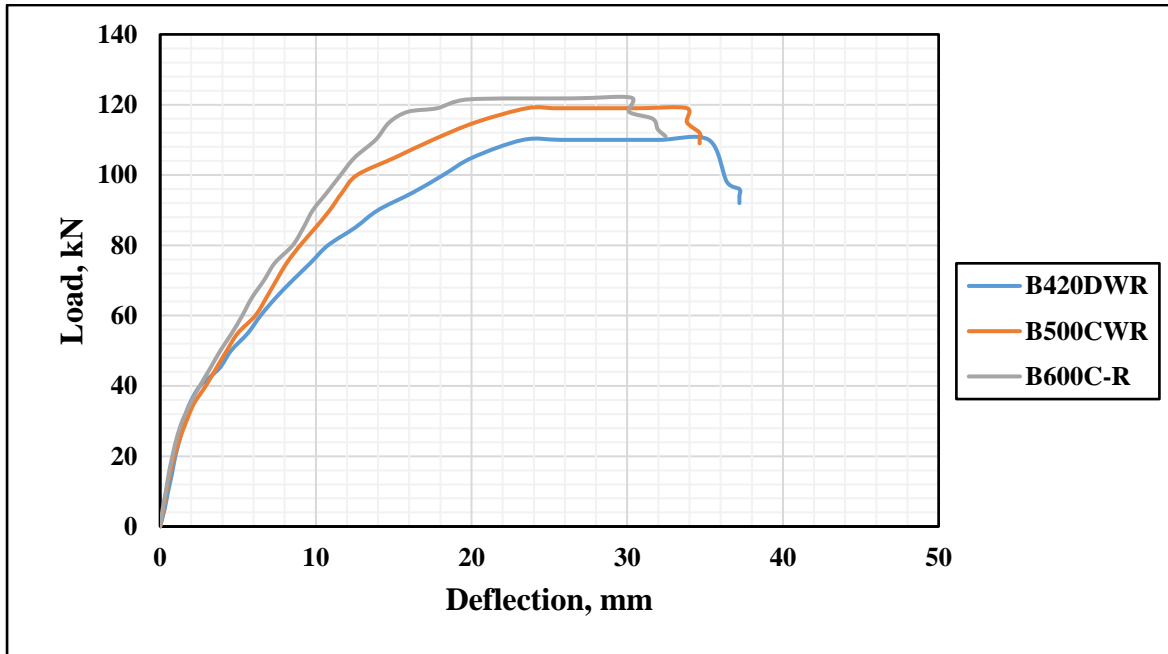


Figure 3.27: Load vs deflection curve of beams for 17.2 MPa (2500 Psi) concrete

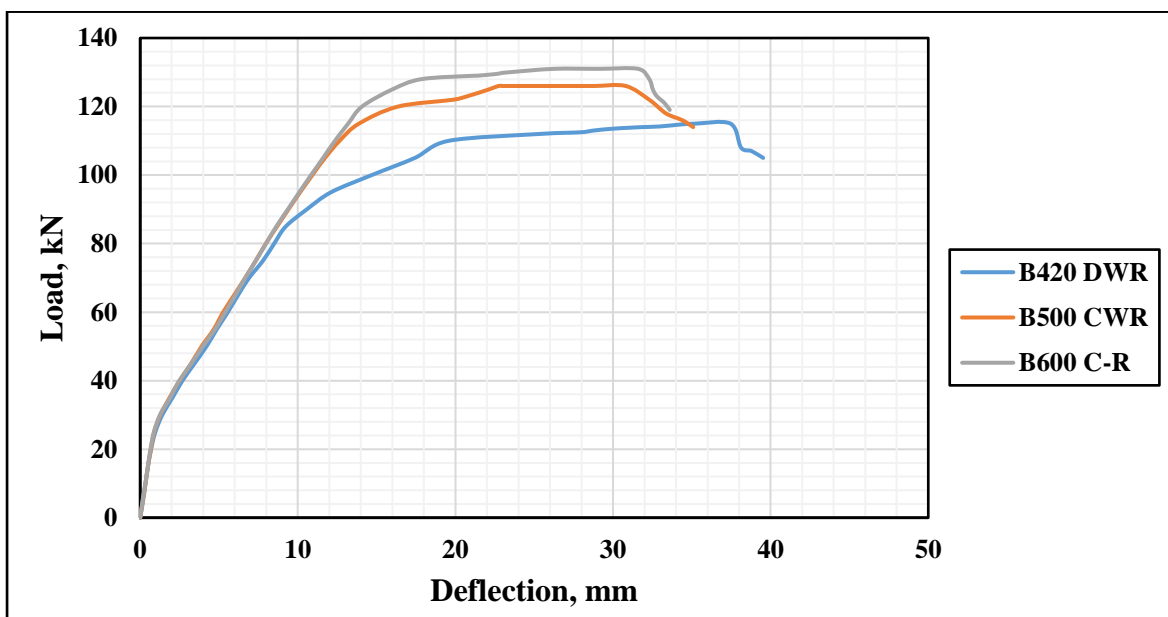


Figure 3.28: Load vs deflection curve of beams for 24.1 MPa (3500 psi) concrete

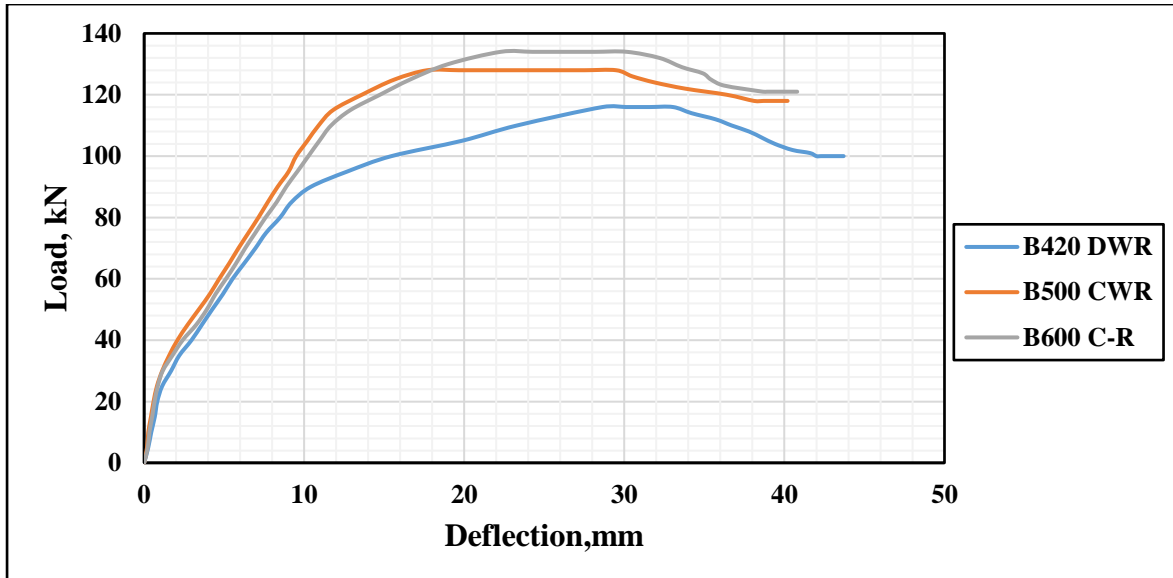


Figure 3.29: Load vs deflection curve of beams for 29.3 MPa (4250 psi) concrete

3.5 Experimental Study of Column

A Universal Testing Machine (UTM) with 1500 kN loading capacity was used for testing of all the column samples. The UTM actuator, which is connected to a movable crosshead, can adjust the stroke rate and applies a compressive force from above. The data collection system made use of a computer running Horizon data acquisition software. Axial Load was applied to the column at the rate of 5 kN/sec. During testing of each specimen, the digital readings of axial load and axial deformation were obtained using an electronic data acquisition system. A schematic diagram of column test setup is shown in Figure 3.30.

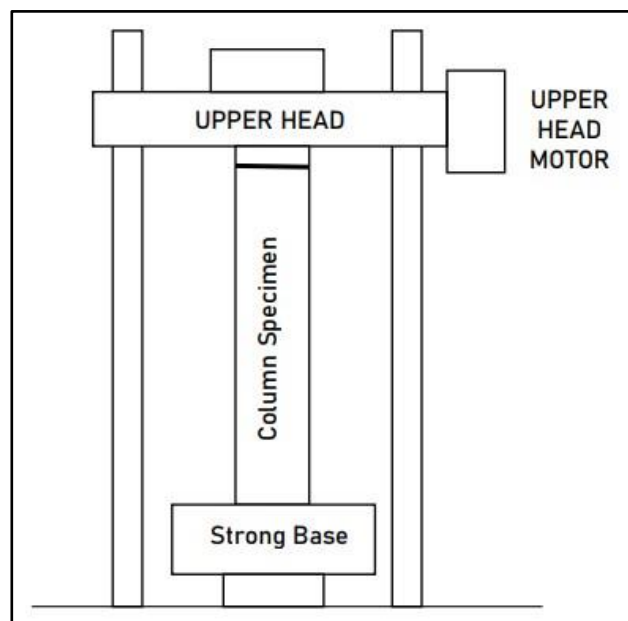


Figure 3.30: Schematic diagram of test setup of column

The columns were so placed in the UTM to provide uniform bearing and a fixed end condition. The specimen was first centered below the UTM actuator. Then the column was vertically oriented. There was enough gap between the machine and the column top before compressive load were applied. A constant load rate of 5 kN/sec was employed for these columns throughout the loading process. The axial load and axial shortening of the test columns were recorded. The point of ultimate failure was usually characterized by the concrete crushing and softening. Nine columns were tested under concentric axial load to evaluate the load versus deformation behavior of the columns. Different grade of steel and concrete mix was used for this column construction. Axial compressive load and axial deformation at the ultimate load were observed.



Figure 3.31: Test set up of column for concentric axial load in laboratory

3.5.1 Column Test Results

Column is a compression member. Strength of column is mainly governed by concrete strength. However, steel strength also influences the strength of column. Higher grade steel increases the column load capacity significantly. From the experiment it is evident that, in combination with lower grade concrete higher grade steel increases load capacity more prominently. One of the reasons of this phenomenon is when cast with lower grade concrete steel takes up the major

share of the load capacity. When higher grade steel is used with higher grade concrete, concrete takes up the major share of load capacity. Experimental test results of column are shown in Table 3.6.

Table 3.6: Experimental test results of column

Column Dimension	Concrete Strength, MPa(Psi)	Steel Grade, MPa	Experimental Capacity, kN	Design Capacity, kN	Remarks
200X200	17.2 (2500)	420	1027	592.03	Satisfactory
		500	1102	633.86	Satisfactory
		600	1208	686.13	Satisfactory
	24.1 (3500)	420	1176	741.46	Satisfactory
		500	1216	783.28	Satisfactory
		600	1262	835.55	Satisfactory
	29.3 (4250)	420	1156	854.07	Satisfactory
		500	1337	895.89	Satisfactory
		600	1365	948.16	Satisfactory

3.5.2 Cracking Characteristics and Failure Patterns of Column

The Cracks formed in the specimen after certain amount of load is applied. Cracking characteristics and failure patterns of the specimens are shown in figure 3.32 to 3.37. Column failure is governed by compressive strength of concrete. However, Strength of steel also influence the failure load and failure pattern.



Figure 3.32: Failure patterns of column reinforced with (a) B420DWR (b) B500CWR



Figure 3.33: Failure patterns of column reinforced with B600C-R



Figure 3.34: Failure patterns of column reinforced with (a) B420DWR (b) B500CWR



Figure 3.35: Failure patterns of column reinforced with B600C-R



Figure 3.36: Failure patterns of column reinforced with (a) B420DWR (b) B500CWR



Figure 3.37: Failure patterns of column reinforced with B600C-R

3.5.3 Load vs Deformation Patterns of Column

Load vs deformation curves for column reinforced with different steel grades are plotted in Figures 3.38 to 3.40. From these graphs it is visible that load capacity of column reinforced with B600C-R is higher than columns reinforced with B420DWR and B500CWR. Although column is a compression member, use of higher strength steel increases the load capacity significantly. Deformation increases with the increase of load and when concrete crushes load decreases abruptly.

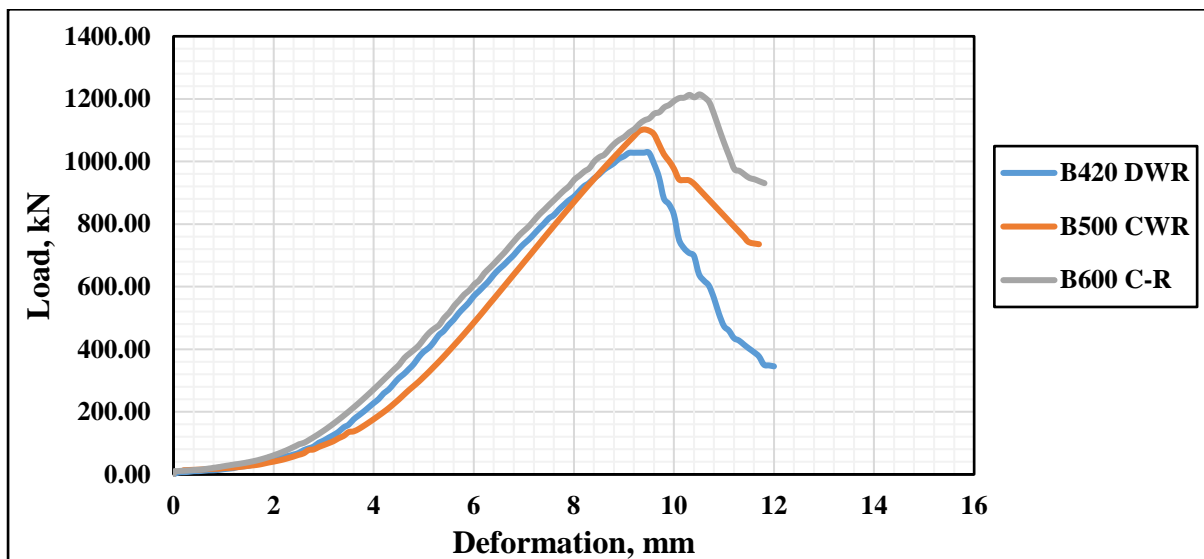


Figure 3.38: Load vs deformation curves of columns for 17.2 MPa concrete

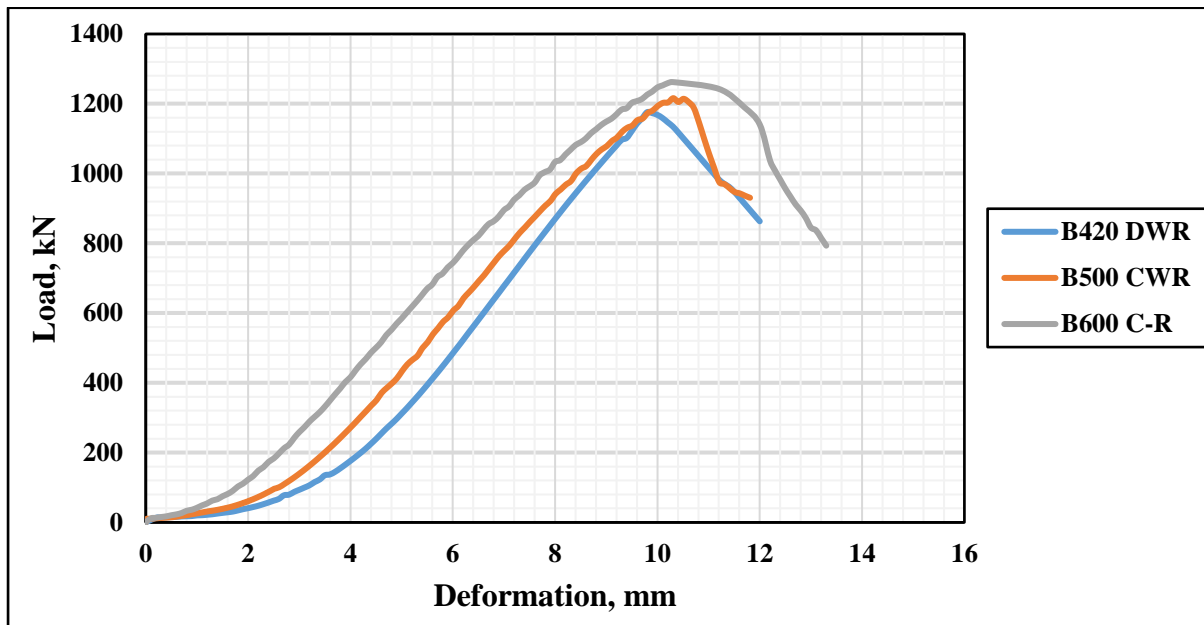


Figure 3.39: Load vs deformation curves of columns for 24.1 MPa concrete

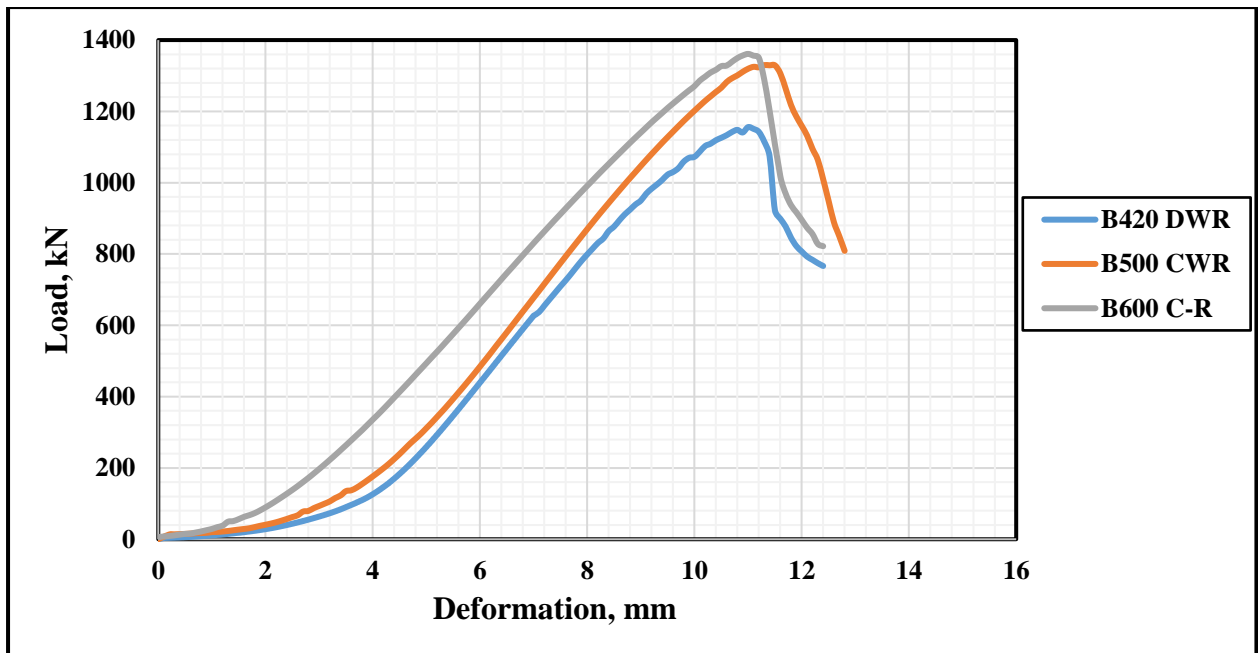


Figure 3.40: Load vs deformation curves of columns for 29.3 MPa concrete

3.6 Experimental Study of Joint

Joint tests were conducted in the concrete laboratory of Department of Civil Engineering, BUET. For ease of testing, the specimens were rotated 90 degrees. The specimen's bottom was supported by rollers and these rollers were put on top of steel boxes. These steel boxes were bolted with the strong floor. Cyclic loading have been applied to the specimen using a push-pull jack. The column has been kept under constant axial compression with the help of a hydraulic jack. The arrangement is shown in Figure 3.41.

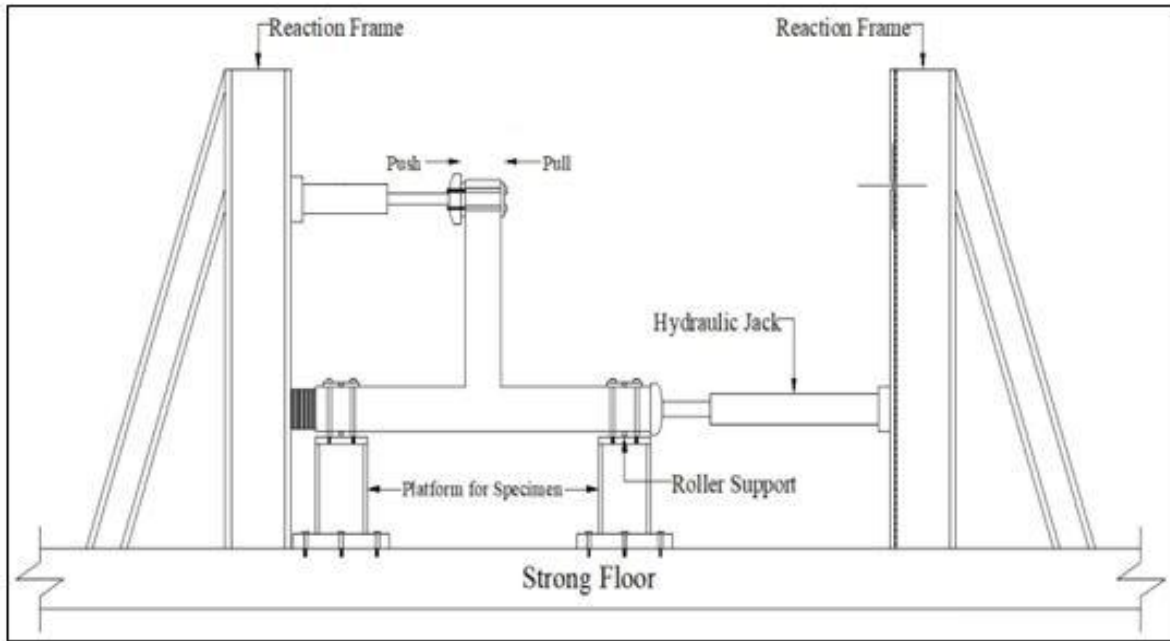


Figure 3.41: Schematic diagram of experimental setup of joint

To measure displacements at three different positions deflection dial gauges were attached as shown in Figure 3.42.

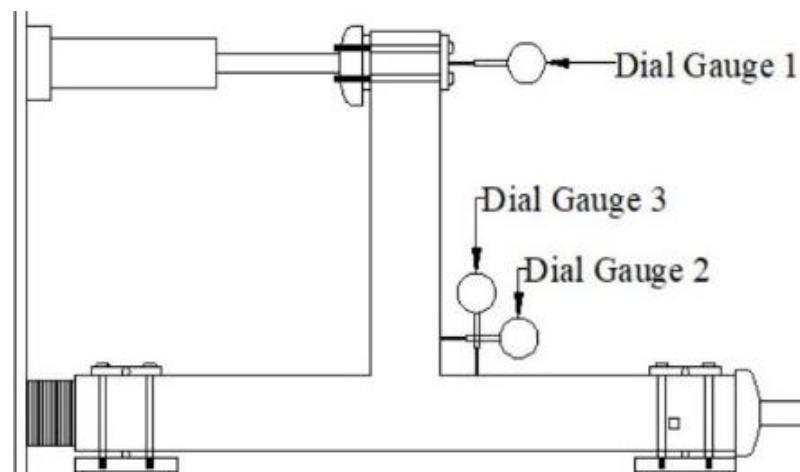


Figure 3.42: Dial gauge positions of joint test

3.6.1 Loading Protocol

Push pull cyclic loading has been applied to the specimen using a hydraulic jack.

This jack was calibrated using load cell.

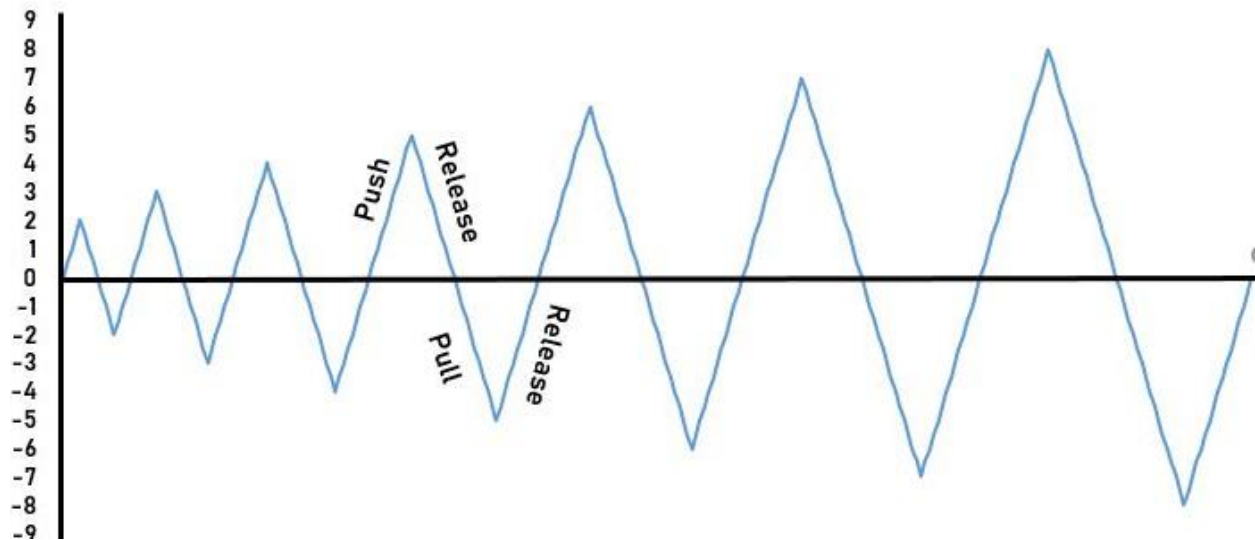


Figure 3.43: Loading protocol of joint test

The column specimens have been kept under compression load. The applied forces are shown in the Table 3.7.

Table 3.7: Axial Forces Applied on Columns

Concrete Strength, f_c , MPa	Gross Area of Joint A_g , mm^2	Axial Force Applied on Column ($0.1 \cdot f_c \cdot A_g$), kN
17.2	90000	155
24.1	90000	217
29.3	90000	264

3.6.2 Joint Test Results

Beam-column joints reinforced with B600C-R can sustain more lateral load. For Higher grade steel number of cycles is also higher. This signifies that higher grade steel performs better in earthquake load. When B600C-R is cast with 17.2 MPa concrete it can take only 6 cycle load. However, when concrete strength increases load capacity and number of cycles also increases. Results of joint test are shown in Table 3.8.

Table 3.8: Experimental test results of Joint

Concrete Strength, MPa (Psi)	Steel Grade, MPa	Cycle Number	Experimental Load Capacity, kN
17.2 (2500)	420	5	45.46
	500	6	52.9
	600	6	52.9
24.1 (3500)	420	5	45.46
	500	6	52.9
	600	7	60.39
29.3 (4250)	420	5	45.46
	500	6	52.9
	600	7	60.39

3.6.3 Cracking Characteristics and Failure Patterns of Joint

After each cycle specimen has been observed closely to identify the formation of any cracks. In some specimens, cracks start to appear after the 2nd cycle. However, for most of the specimens, cracks became visible after the 3rd cycle. Figures 3.44 to 3.48 shows the cracking characteristics of joints for different steel grades and concrete classes. Each crack was marked with a black marker and it was given a number which indicates the cycle number. The test was continued until the specimen failed to sustain any more lateral load.

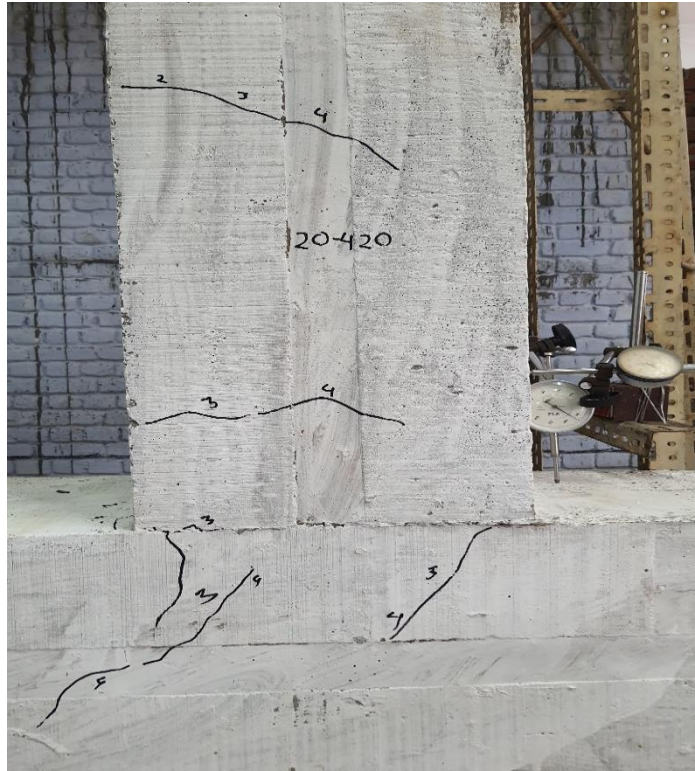


Figure 3.44: Cracking characteristics of joint reinforced with B420DWR

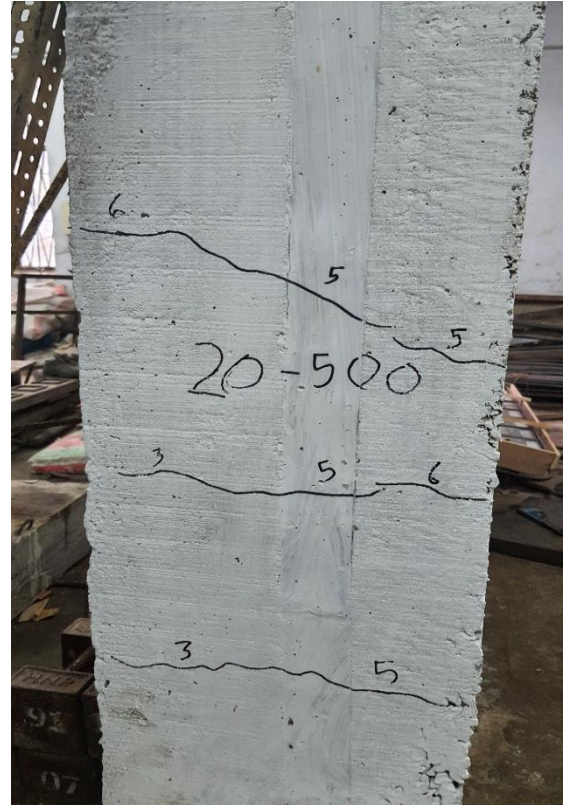
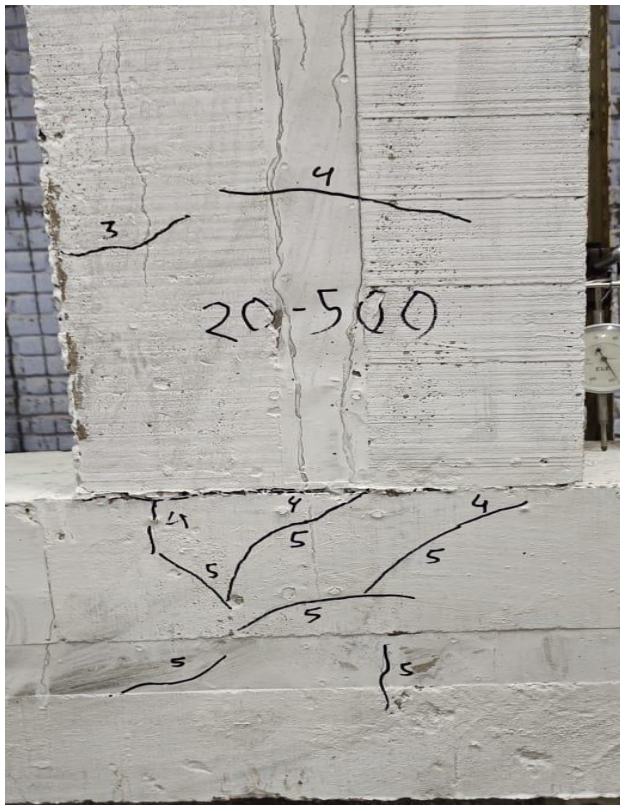


Figure 3.45: Cracking characteristics of joint reinforced with B500CWR

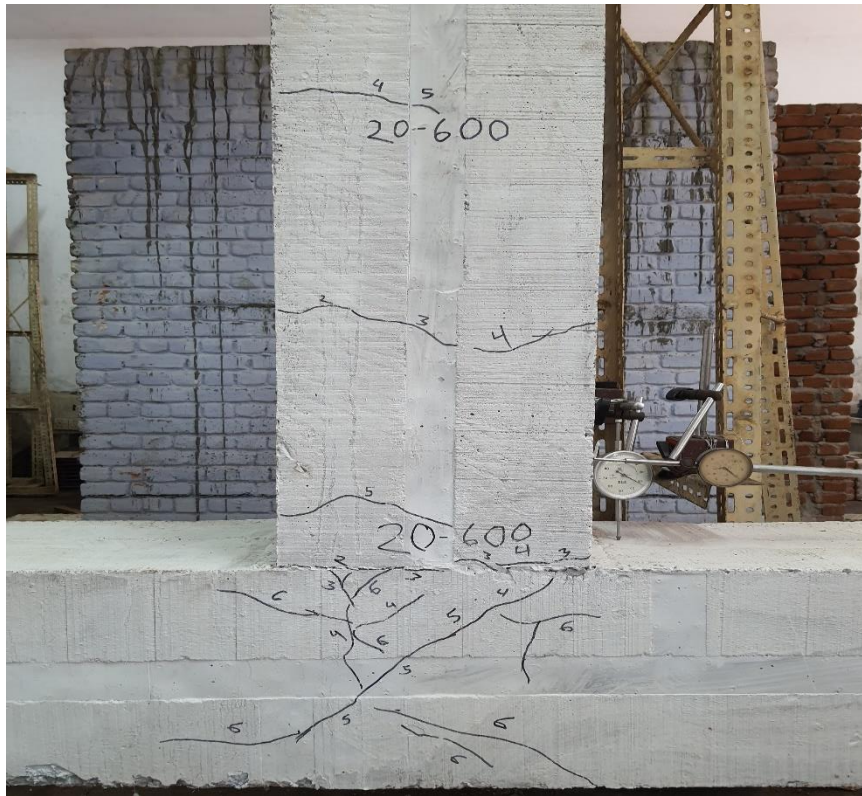


Figure 3.46: Cracking characteristics of joint reinforced with B600C-R



Figure 3.47: Cracking characteristics of joint reinforced with (a) B420DWR (b) B500CWR



Figure 3.48: Cracking characteristics of joint reinforced with B600C-R

3.6.4 Load- Displacement Response of Joint

Figures 3.49 to 3.57 shows the load-displacement response of joints for different steel grade and concrete classes. The curves in each cycle have been colored differently for ease of understanding.

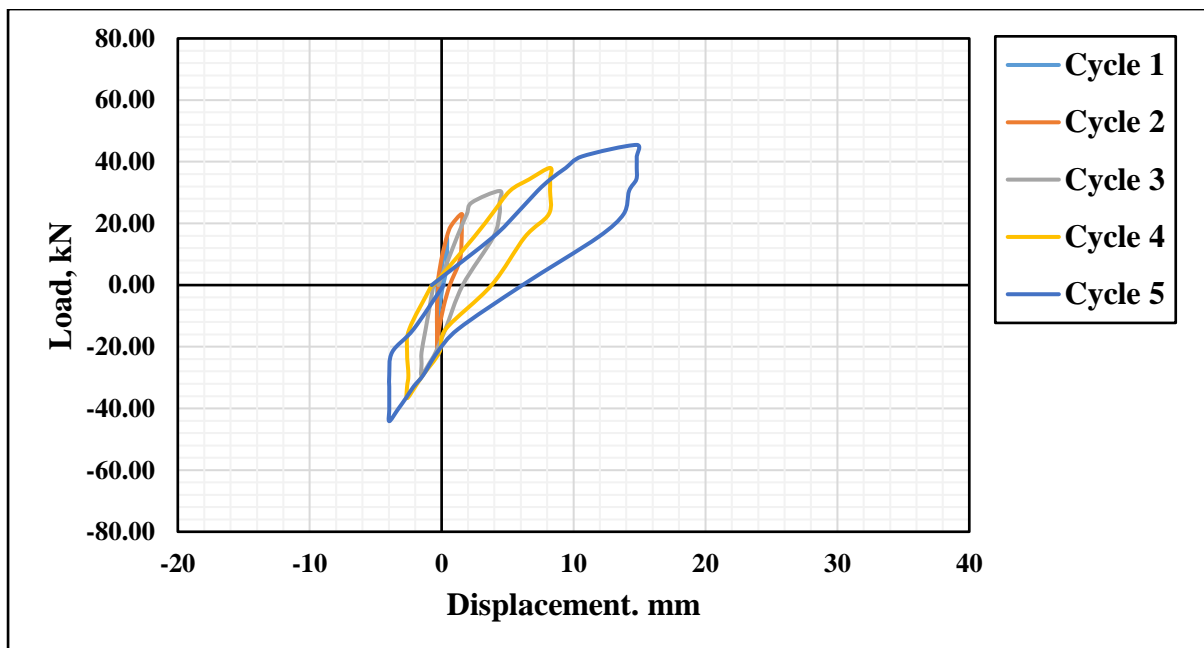


Figure 3.49: Load-Displacement Response of Joint Reinforced with B420DWR and cast with 17.2 MPa concrete

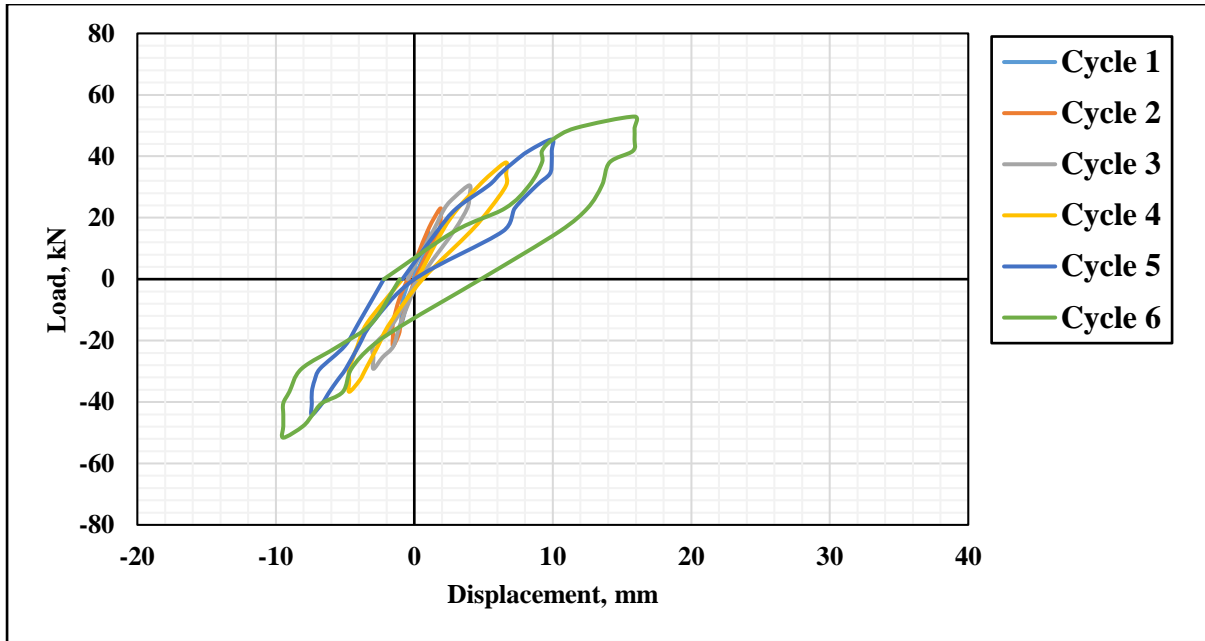


Figure 3.50: Load-Displacement Response of Joint Reinforced with B500CWR and cast with 17.2 MPa concrete

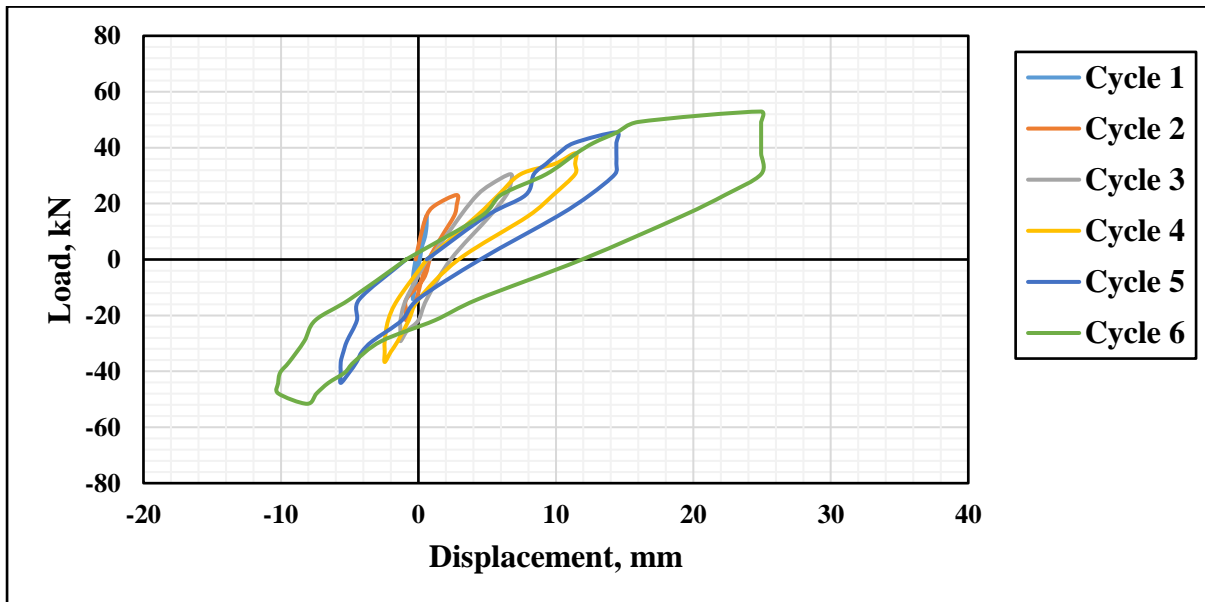


Figure 3.51: Load-Displacement Response of Joint Reinforced with B600C-R and cast with 17.2 MPa concrete

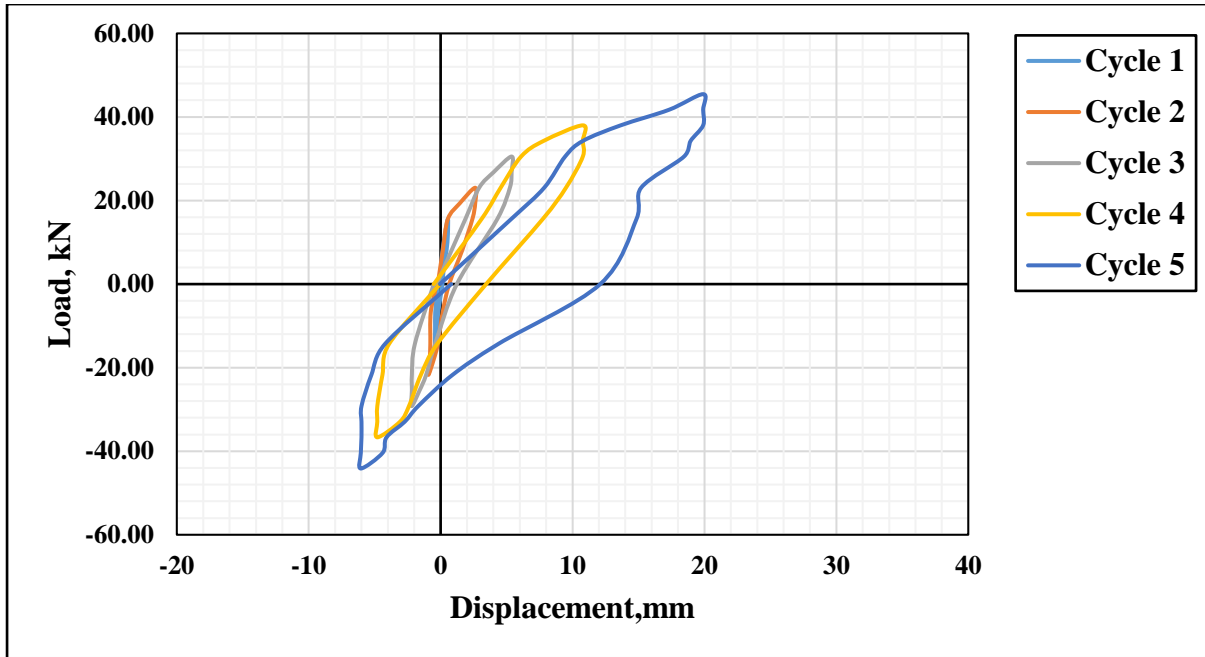


Figure 3.52: Load-Displacement Response of Joint Reinforced with B420DWR and cast with 24.1 MPa concrete

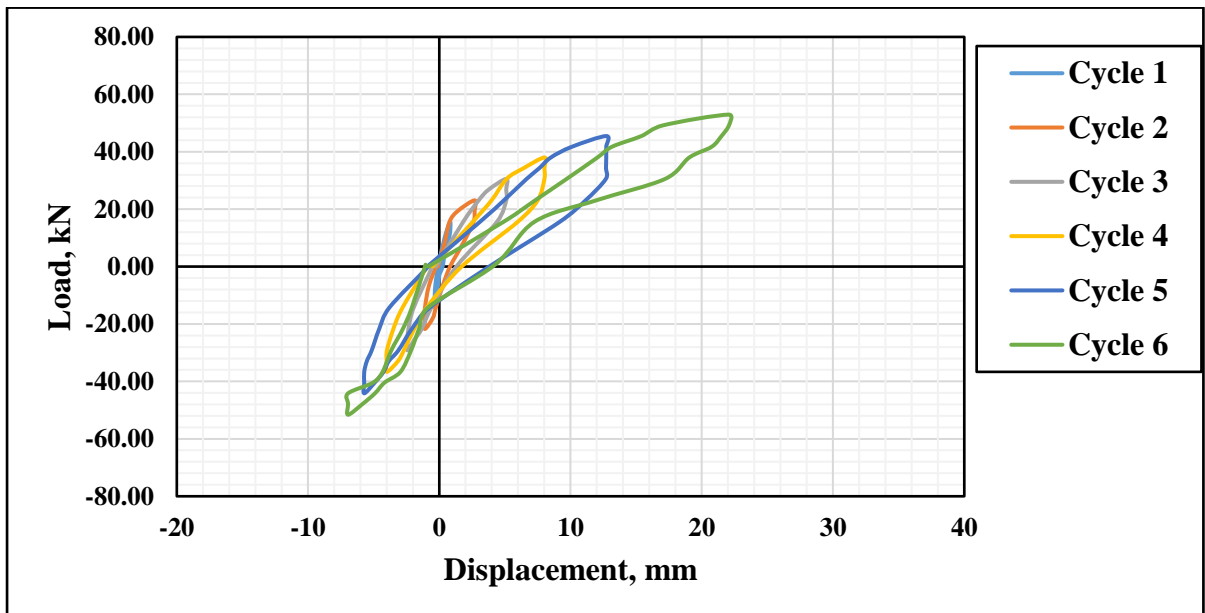


Figure 3.53: Load-Displacement Response of Joint Reinforced with B500 CWR and cast with 24.1 MPa concrete

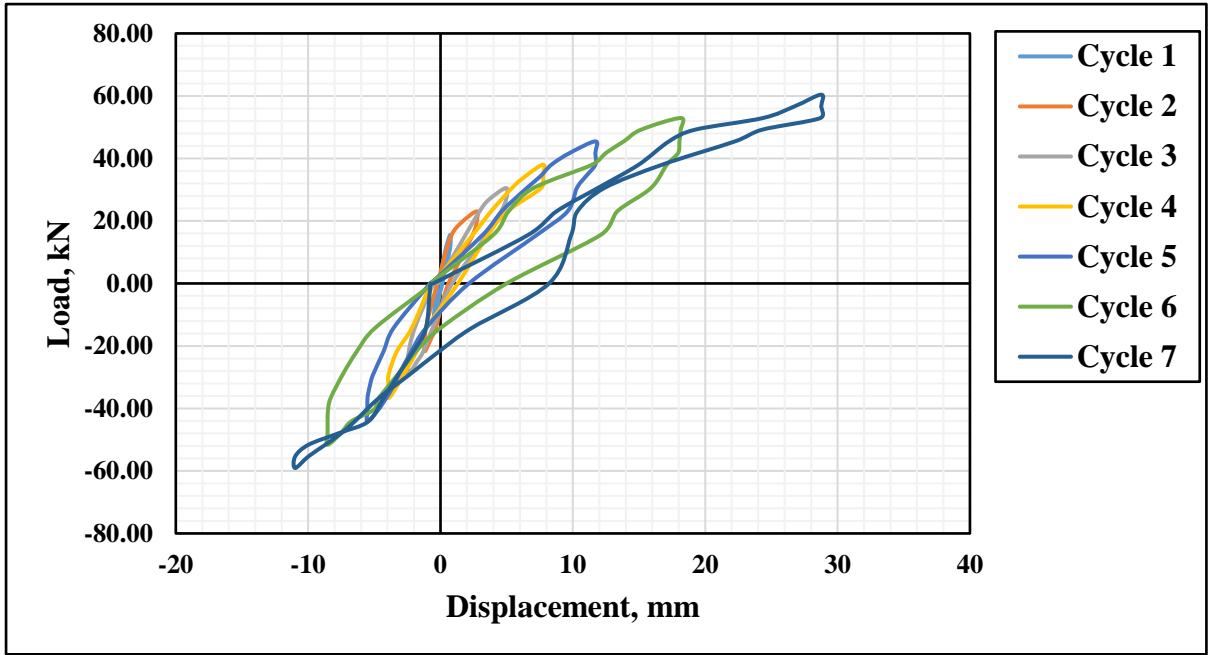


Figure 3.54: Load-Displacement Response of Joint Reinforced with B600 C-R and cast with 24.1 MPa concrete

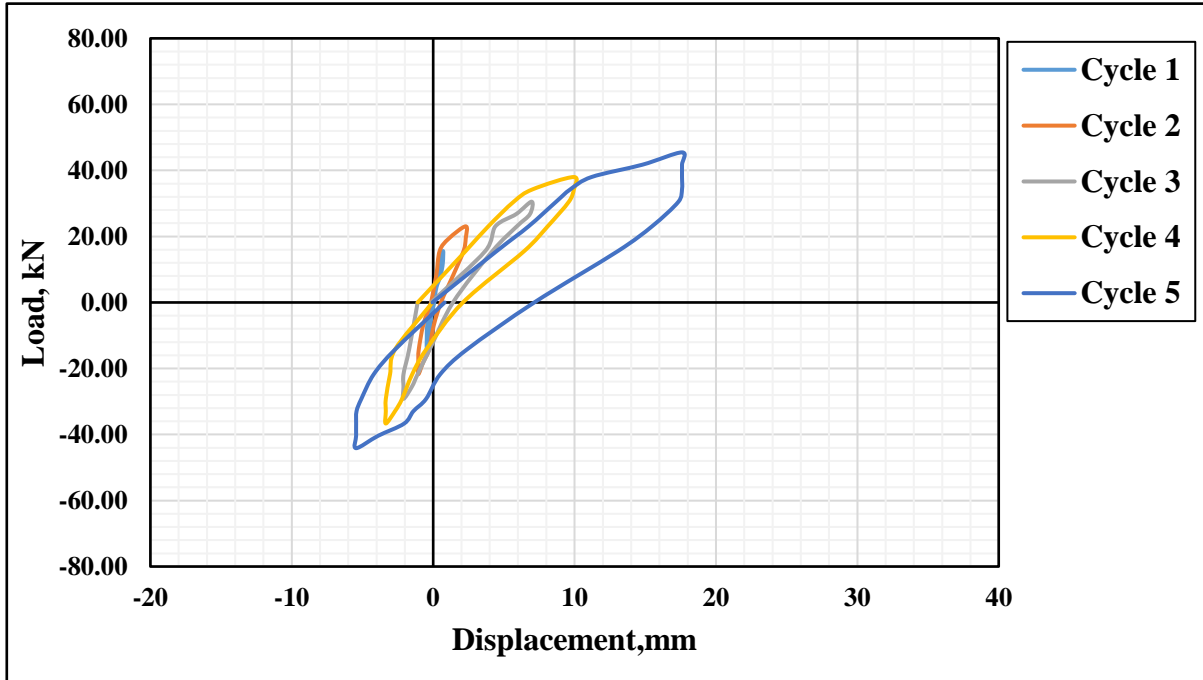


Figure 3.55: Load-Displacement Response of Joint Reinforced with B420 DWR and cast with 29.3 MPa concrete

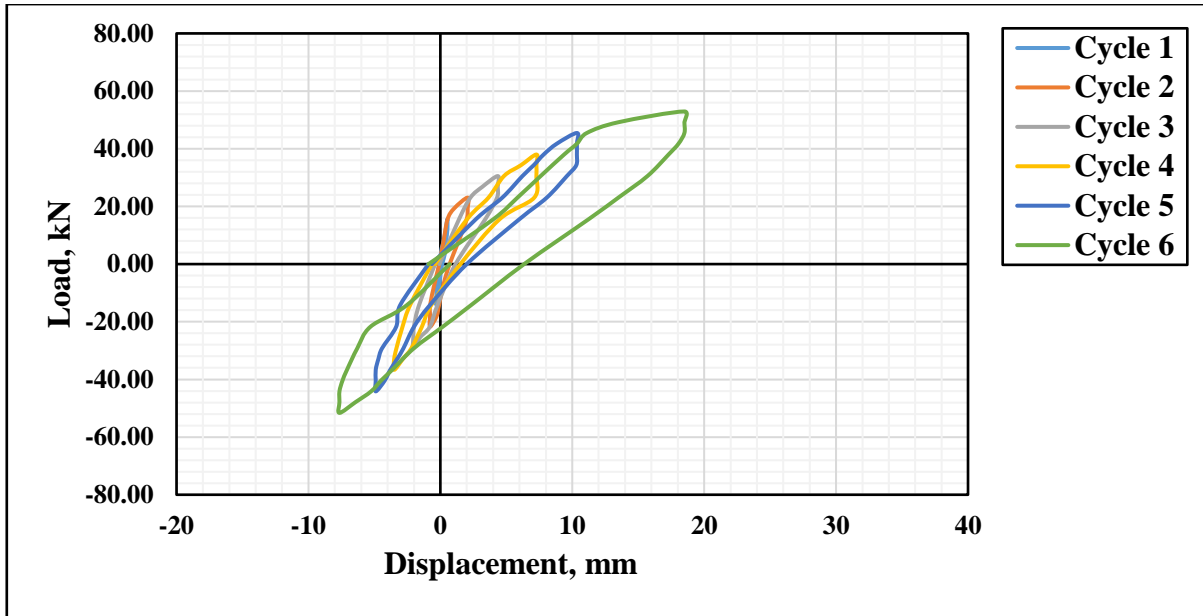


Figure 3.56: Load-Displacement Response of Joint Reinforced with B500 CWR and cast with 29.3 MPa concrete

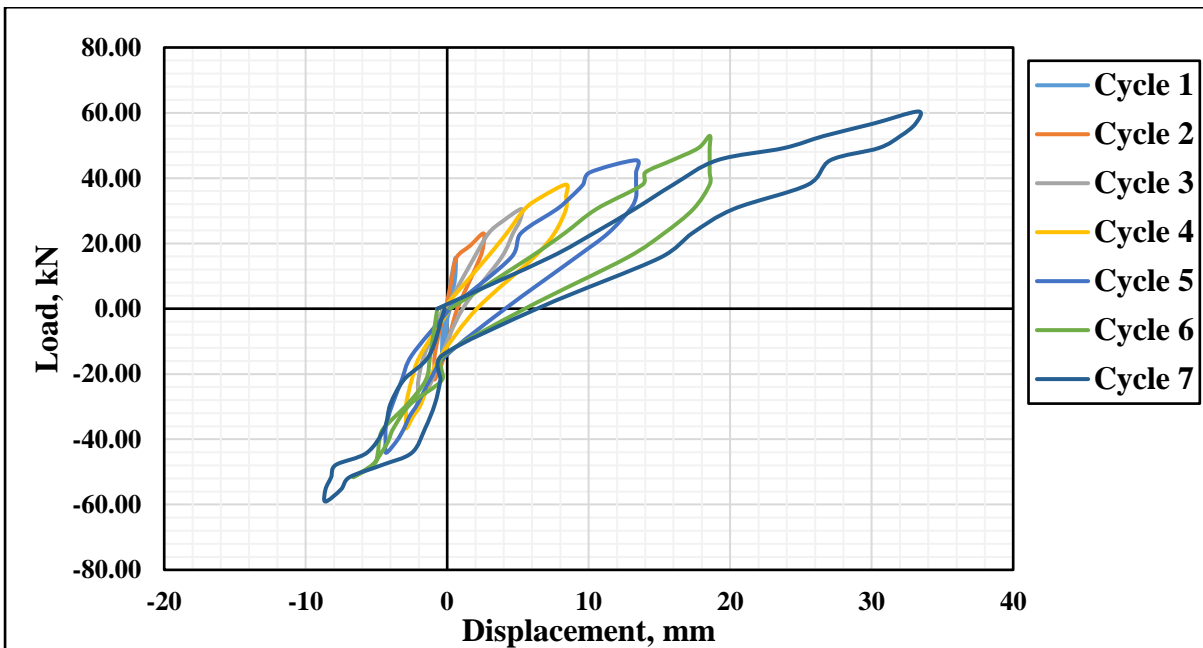


Figure 3.57: Load-Displacement Response of Joint Reinforced with B600 C-R and cast with 29.3 MPa concrete

3.6.4 Stiffness Degradation

Stiffness of a joint can be calculated by joining the peak points of forward and reverse half cycle. Calculated stiffness is plotted to determine the stiffness degradation patterns of specimens as shown from Figures 3.58 to 3.66.

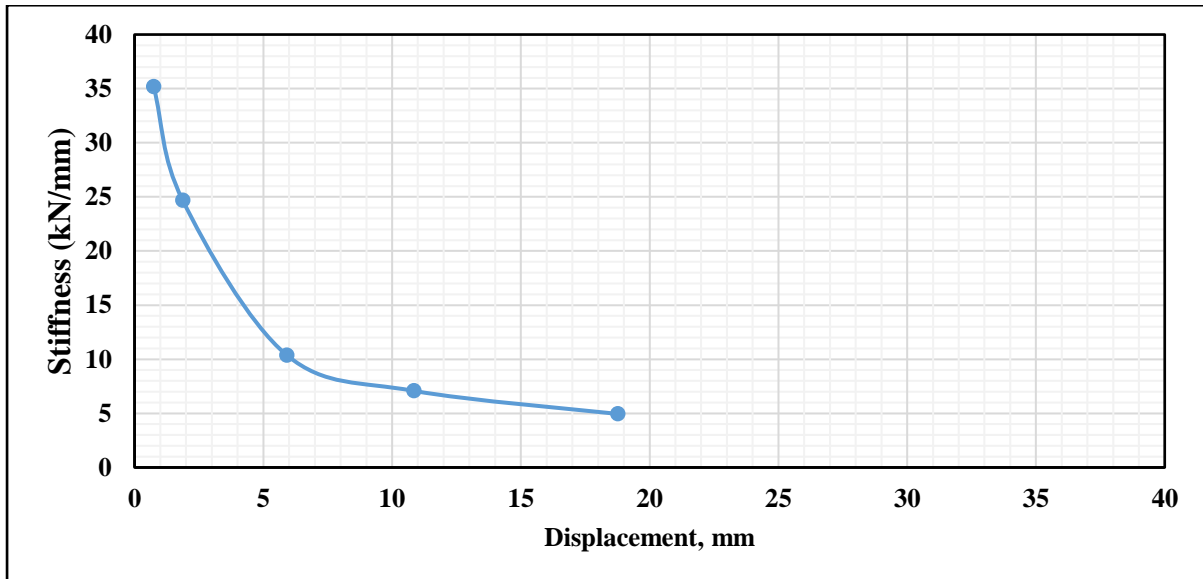


Figure 3.58: Stiffness degradation curve of joint reinforced with B420DWR and cast with 17.2 MPa concrete

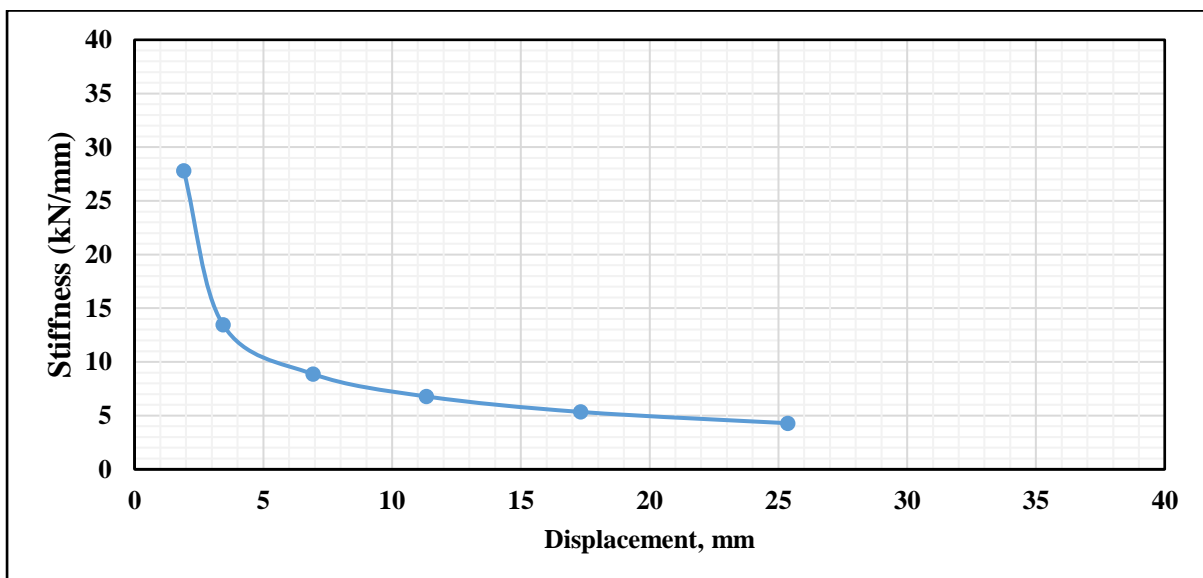


Figure 3.59: Stiffness degradation curve of joint reinforced with B500CWR and cast with 17.2 MPa concrete

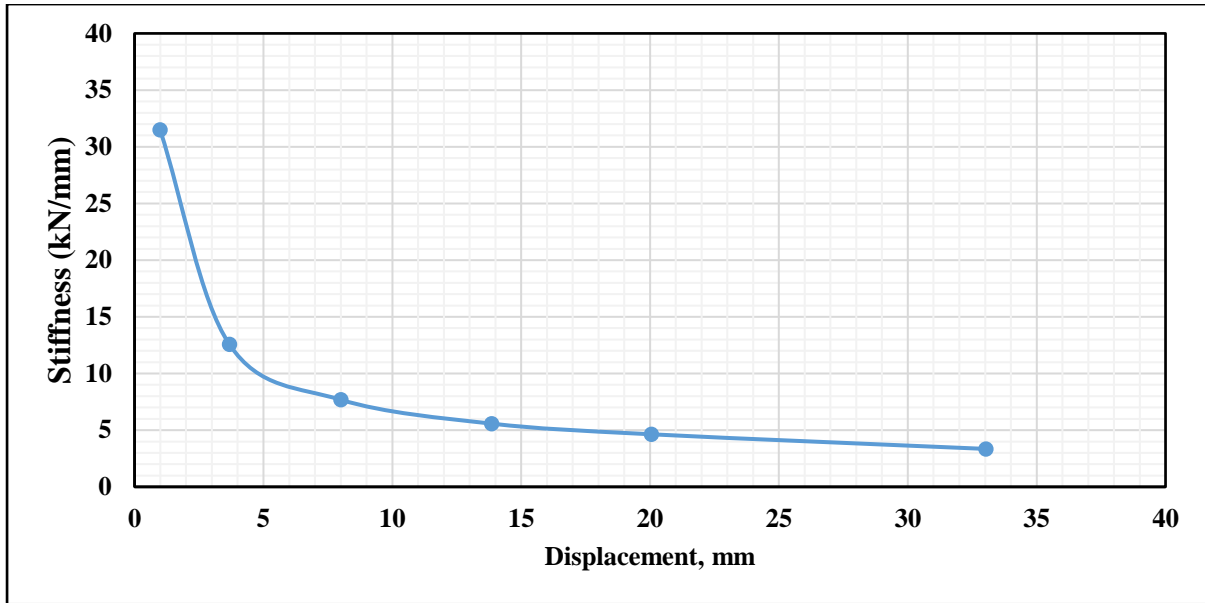


Figure 3.60: Stiffness degradation curve of joint reinforced with B600C-R and cast with 17.2 MPa concrete

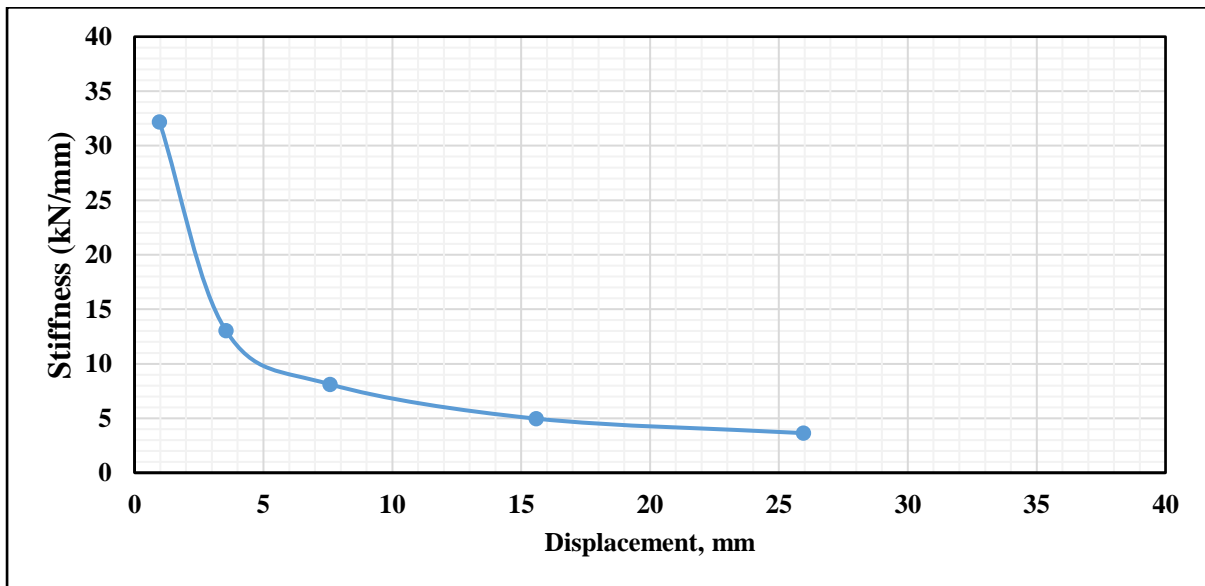


Figure 3.61: Stiffness degradation curve of joint reinforced with B420DWR and cast with 24.1 MPa concrete

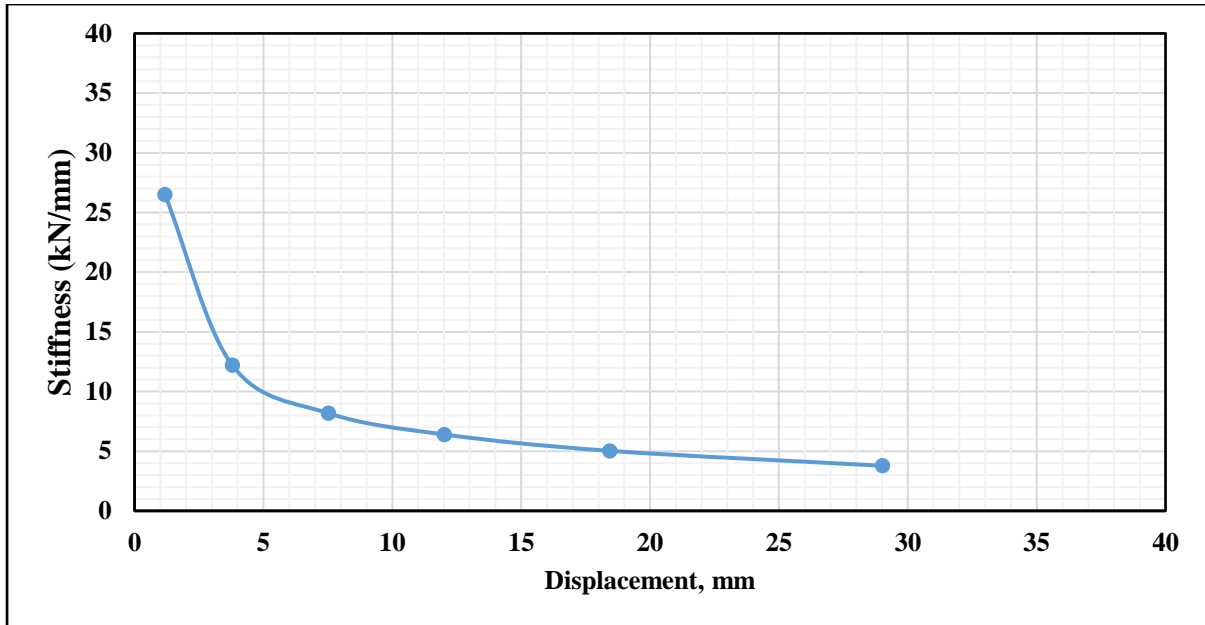


Figure 3.62: Stiffness degradation curve of joint reinforced with B500CWR and cast with 24.1 MPa concrete

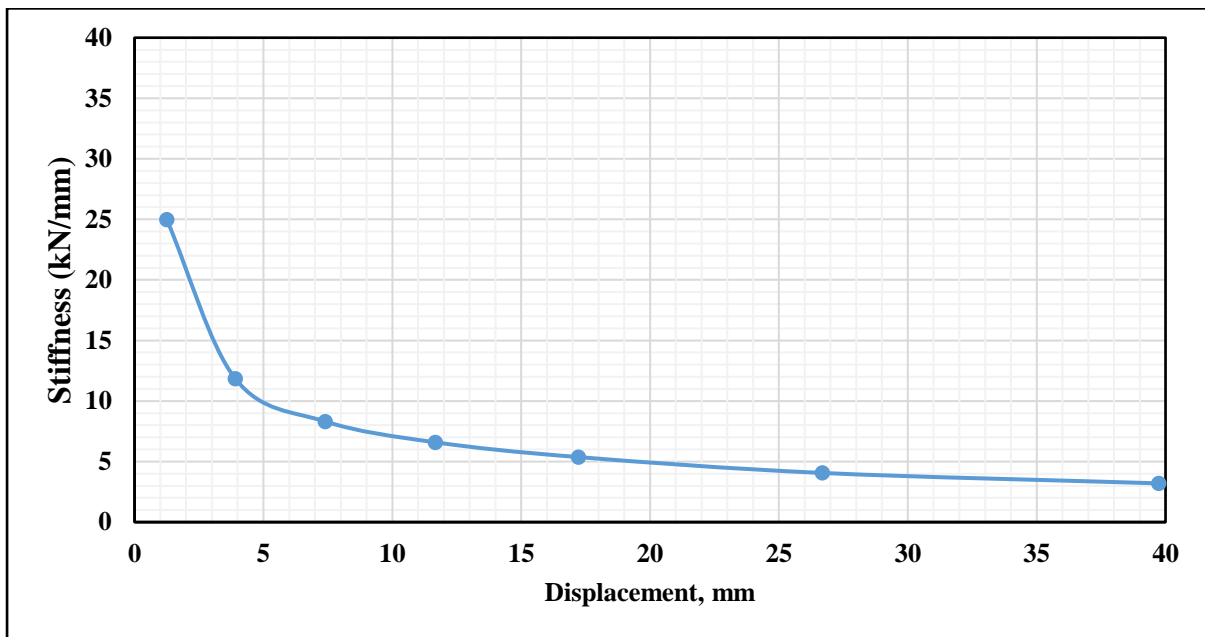


Figure 3.63: Stiffness degradation curve of joint reinforced with B600C-R and cast with 24.1 MPa concrete

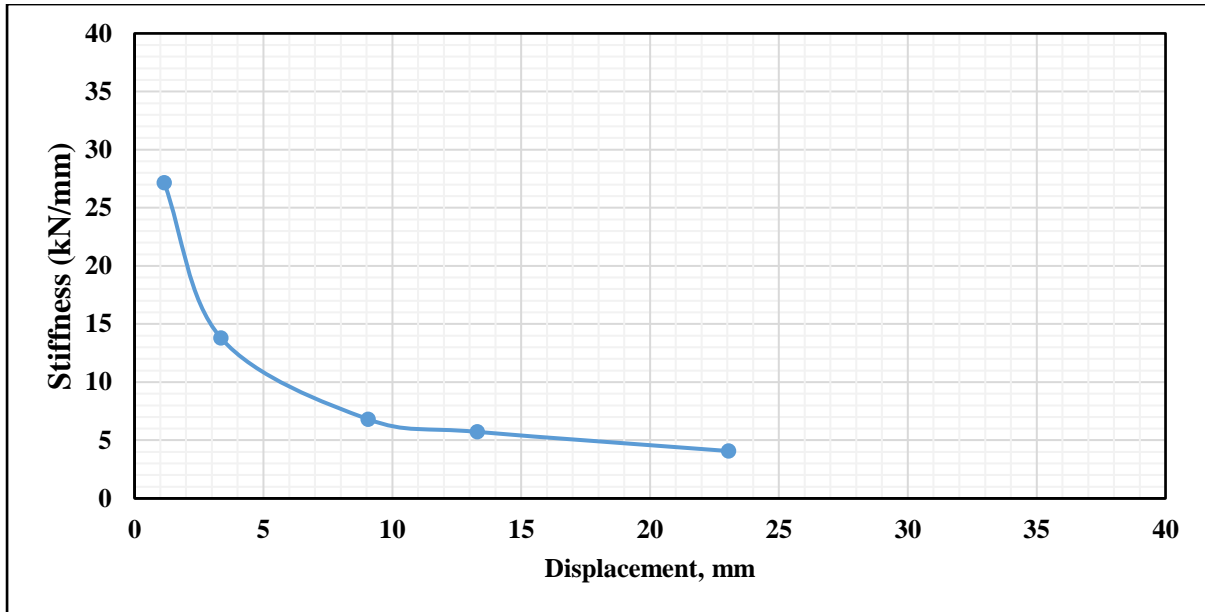


Figure 3.64: Stiffness degradation curve of joint reinforced with B420DWR and cast with 29.3 MPa concrete

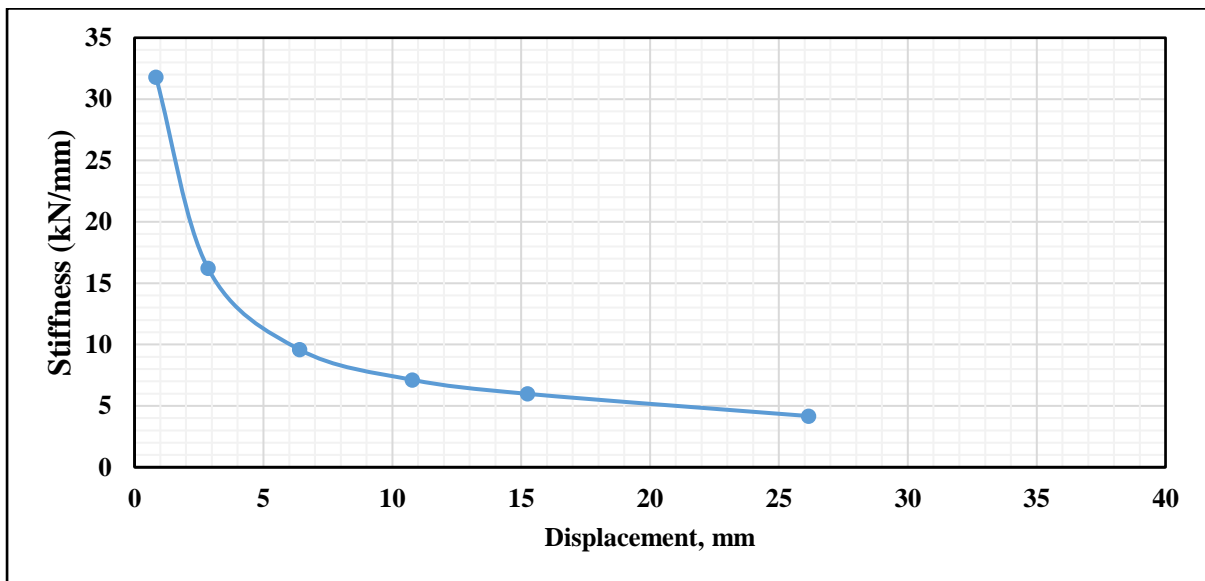


Figure 3.65: Stiffness degradation curve of joint reinforced with B500CWR and cast with 29.3 MPa concrete

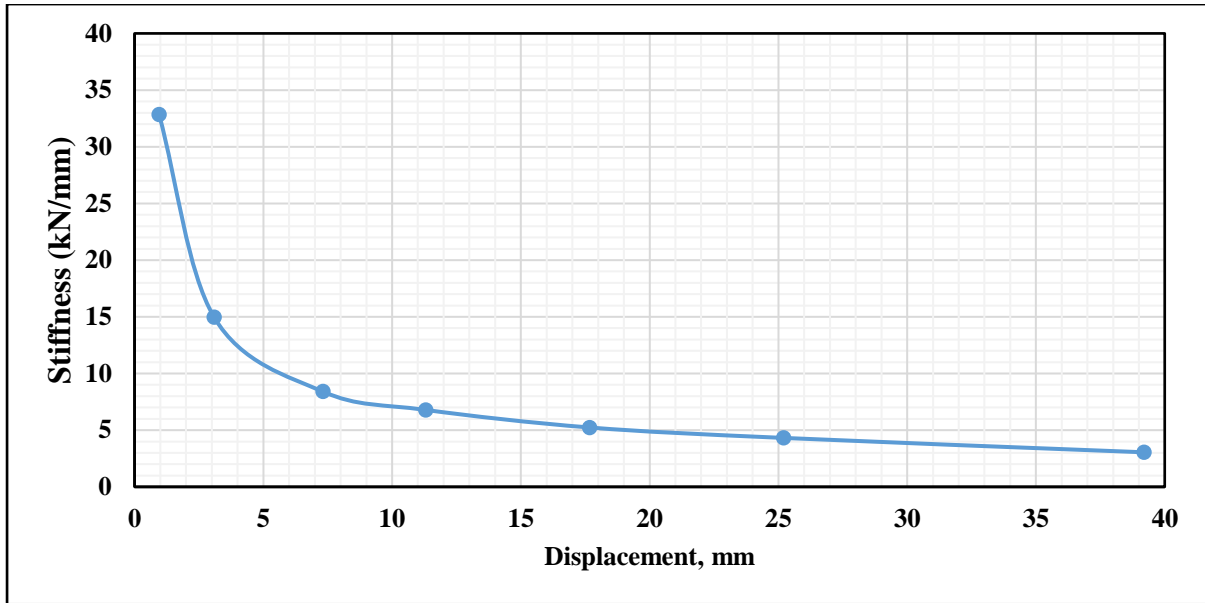


Figure 3.66: Stiffness degradation curve of joint reinforced with B600C-R and cast with 29.3 MPa concrete

CHAPTER 4 DESIGN COMPARISONS

4.1 Beam Design Comparisons

A beam with a span length of 5m is designed for different steel grades and concrete classes. Section of the beam is assumed to be 375X300 mm and the uniformly distributed load on the beam is considered to be 72kN/m. Bending Moment Diagram for this beam section is shown in Figure 4.1.

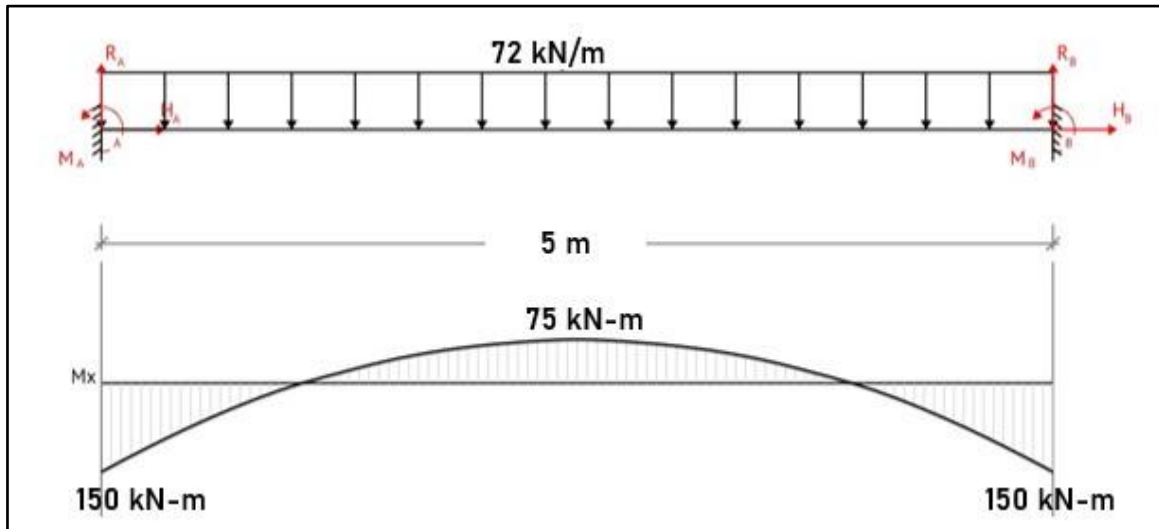


Figure 4.1: Bending Moment Diagram of Beam

The beam was designed to resist this 150 kN-m bending moment for different grades of steel and concrete classes as shown in Table 4.1.

Table 4.1: Steel consumption comparison in beam for different grades of steel

Design Moment, kN-m	Beam Dimension, mm	Effective Depth, mm	Yield Strength of Steel, MPa	Compressive Strength of Concrete, MPa(Psi)	Required Steel Area, mm ²	Savings of Steel Consumptions
150	375X300	335	420	17.2 (2500)	1510.76	0%
			500		1269.04	16% w.r.t B420
			600		1057.53	30% w.r.t B420 16.7% w.r.t B500
			420	24.1 (3500)	1378.34	0%
			500		1157.81	16% w.r.t B420
			600		964.84	30% w.r.t B420 16.7 w.r.t B500
			420	29.3 (4250)	1333.82	0%
			500		1120.41	16% w.r.t B420
			600		933.67	30% w.r.t B420 16.7 w.r.t B500

While providing reinforcements according to the requirements, saving percentage will change slightly. In Table 4.2 required steel area is provided with different diameter of rebar to optimize the cost for using higher grade.

Table 4.2: Steel consumption comparison in beam after providing rebar

Yield Strength of Steel, MPa	Compressive Strength of Concrete, MPa	Required Steel Area, mm ²	Provided Steel	Provided Steel Area,mm ²	Savings of Steel Consumptions
420	17.2 (2500)	1510.76	2-25mm & 2-20 mm	1610	0%
500		1269.04	2-25 mm & 1-20 mm	1296	19.5% w.r.t B420
600		1057.53	2-25 mm & 1-16 mm	1183	26.5% w.r.t B420 8.7% w.r.t B500
420	24.1 (3500)	1378.34	2-25 mm & 2-16 mm	1384	0%
500		1157.81	2-25 mm & 1-16 mm	1183	14.5 % w.r.t B420
600		964.84	2-25 mm	982	29.0% w.r.t B420 16.9% w.r.t B500
420	29.3 (4250)	1333.82	2-25 mm & 2-16 mm	1384	0%
500		1120.41	2-25 mm & 1 -16 mm	1183	14.5 %w.r.t B420
600		933.67	3-20 mm	942	31.9% w.r.t B420 20.4% w.r.t B500

From Table 4.2, it is visible that steel consumption reduces significantly when higher grade steel is used. However, this reduction in consumption is not fixed. It varies according to design. Also, Reinforcements are available in only certain diameters. So, while providing steel sometimes engineers have to provide much higher quantity due to unavailability of rebar size. Finally, it can be said that reduction in steel consumption mainly depends on the design of the structure, section size and availability of required size of rebar.

4.2 Column Design Comparisons

An interior column with a span length 5m on both sides, is designed using different concrete classes and steel grades. 200 Psf load is considered on the column tributary area.

4.2.1 Column Design of 8 Story Building

Variation of required steel area and cost saving percentage have been calculated for an interior column situated in the ground floor of a 8 story(G+7) building.

Table 4.3: Steel consumption comparison in column for different grades of steel

Design Load, kN	Column Section, mm	Ag,mm ²	Compressive Strength of Concrete, MPa	Yield Strength of Steel, MPa	Required steel Area, mm ²	Savings of Steel Consumptions
2000	375X375	140625	13.8	420	5380.318	0%
				500	4498.787	16.4% w.r.t B420
				600	3734.038	30.6% w.r.t B420 16.9% w.r.t B500
			17.2	420	4416.144	0%
				500	3688.278	16.4% w.r.t B420
				600	3058.212	30.8% w.r.t B420 17.1% w.r.t B500
			20.6	420	3438.123	0%
				500	2868.060	16.6% w.r.t B420
				600	2375.680	30.9% w.r.t B420 17.2% w.r.t B500
			24.1	420	2416.557	0%
				500	2013.39	16.7% w.r.t B420
				600	1665.963	31.0% w.r.t B420 17.2% w.r.t B500

Table 4.3 signifies that higher grade steel reduces steel quantity in a certain percentage regardless of concrete strength. However, rebar is only available in certain diameters and also we can provide only even number of rebar for columns. As a result, an engineer sometimes have to provide rebar in much higher quantity than required. These facts change the percentage of steel consumption reduction.

Table 4.4: Steel consumption comparison in column after providing rebar

Compressive Strength of Concrete, MPa	Yield Strength of Steel, MPa	Required steel Area, mm ²	Provided Steel	Provided Steel Area, mm ²	Savings of Steel Consumptions
13.8	420	5380.318	10-25 mm & 2-20 mm	5538	0%
	500	4498.787	8-25 mm & 2-20 mm	4556	17.7% w.r.t B420
	600	3734.038	12-20 mm	3768	31.9% w.r.t B420 17.3% w.r.t B500
17.2	420	4416.144	4-25 mm & 8-20 mm	4476	0%
	500	3688.278	4-25 mm & 6-20 mm	3848	14.0% w.r.t B420
	600	3058.212	4-25 mm & 6-16 mm	3170	29.2% w.r.t B420 17.6% w.r.t B500
20.6	420	3438.123	10-20 mm & 2-16 mm	3542	0%
	500	2868.060	8-20 mm & 2-16 mm	2914	17.7% w.r.t B420
	600	2375.680	12-16 mm	2412	31.9% w.r.t B420 17.2% w.r.t B500
24.1	420	2416.557	8-20 mm	2512	0%
	500	2013.39	4-20 mm & 4-16 mm	2060	17.9% w.r.t B420
	600	1665.963	6-20 mm	1884	25% w.r.t B420 8.5 % w.r.t B500

In Table 4.4, required steel area is provided with different diameter of rebar. As we have to provide even number of rebar in column, change in steel consumption for using higher grade varies significantly. However, in all the cases steel consumption is less for higher grade steel.

4.3 Slab Design Comparisons

A two way slab supported on all four edges is designed for different steel grades.

Design Considerations:

Length of the slab on both direction = 21 ft

Clear Span on both direction = 20 ft

Floor Finish = 50 Psf

Partition Wall = 50 Psf

Live Load = 40 Psf

Compressive strength of concrete = 3000 Psi

Minimum Slab Thickness = $t = \text{Perimeter of slab} \div 180 = 20 * 4 * 12 \div 180 = 5.33 \text{ in}$

Let, Slab Thickness = 6 inch

Self-weight of slab = $(6 \div 12) * 150 \text{ Psf} = 75 \text{ Psf}$

Total Dead Load = 175 Psf

Factored Dead Load $W_{DL} = 1.2 * 175 = 210 \text{ Psf}$

Factored Live Load $W_{LL} = 1.6 * 40 = 64 \text{ Psf}$

Factored load $W_u = 1.2 * DL + 1.6 * LL = 1.2 * 175 + 1.6 * 40 = 274 \text{ Psf}$

$C_a, C_b = \text{Moment Coefficients}$

$M_a = \text{Moment in Short Direction}$

$M_b = \text{Moment in Long Direction}$

Positive Moments in Short Direction $M_a = C_{aDL} * W_{DL} * L_A^2 + C_{aLL} * W_{LL} * L_A^2$

Positive Moments in Long Direction $M_b = C_{bDL} * W_{DL} * L_B^2 + C_{bLL} * W_{LL} * L_B^2$

Negative Moments in short Direction $M_a = C_a * W_u * L_a^2$

Negative Moments in Long Direction $M_b = C_b * W_u * L_b^2$

Here, length is same for both directions. So, there is only one positive moment & one negative moment.

Negative Moment = $0.045 * 274 * 20^2 = 4932 \text{ lb-ft} = 60 \text{ k-in}$

Positive Moment = $0.018 * 210 * 20^2 + 0.027 * 64 * 20^2 = 2203.2 \text{ lb-ft} = 26.4 \text{ k-in}$

A slab is designed to resist this positive & negative moment for different grade of steel and as shown in table 4.5.

Table 4.5: Steel consumption comparison in slab for different grades of steel

Rebar Grade	B420DWR	B500CWR	B600C-R
Negative Moment Reinforcements(in ²)	0.233	0.193	0.161
Positive Moment Reinforcements(in ²)	0.1296	0.107	0.089
Top Bar Spacing	10 mm bar @ 6 in c/c	10 mm bar @ 7.5 in c/c	10 mm bar @ 9 in c/c
Bottom Bar Spacing	10 mm bar @ 11 in c/c	10 mm bar @ 13.5 in c/c	10 mm bar @ 16 in c/c
Top Bar Quantity (kg)	75	60	50
Bottom Bar Quantity(kg)	172.96	142.88	120.32
Total Rebar (kg)	247.96	202.88	170.32
Savings of Steel Consumptions	0%	18.2% w.r.t B420DWR	31.3% w.r.t B420DWR 16.0% w.r.t B500CWR

From Table 4.5, it is evident that use of B600 C-R in slab is economical compared to B420 DWR and B500 CWR.

4.4 Column Interaction Diagram

A column interaction diagram have been prepared for different grade of steel. Compressive strength of concrete is 4000 psi. Section of the column is shown in Figure 4.2.

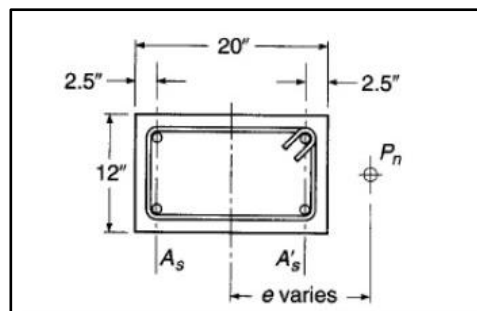


Figure 4.2: Selected column section for interaction diagram

This column is reinforced with four no. 9 bars (28 mm diameter rebar). Strength interaction diagram for this column is shown in Figure 4.3.

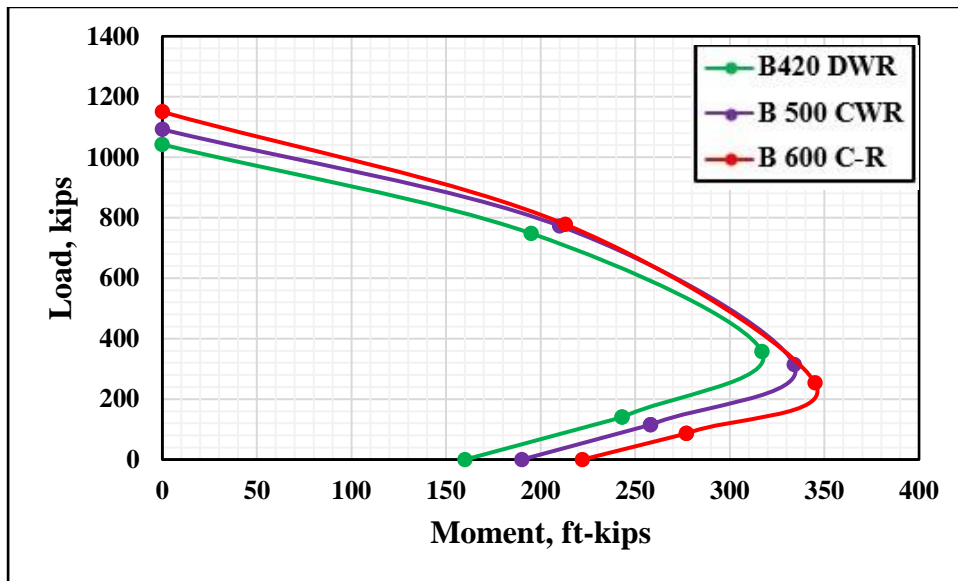


Figure 4.3: Variation of column interaction diagram for B420DWR, B500CWR and B600C-R

4.5 Comparison from Model

A 10 Storied Residential Building has been modeled using ETABS software. This Building has been analyzed using three different grades (B420DWR, B500CWR, B600C-R) of rebar in beams and columns to find out the cost efficiency of using higher grade steel. As higher grade steel will be mainly used for high rise buildings, a 10 storied building has been chosen. 3D view of the selected model is shown in Figure 4.4.

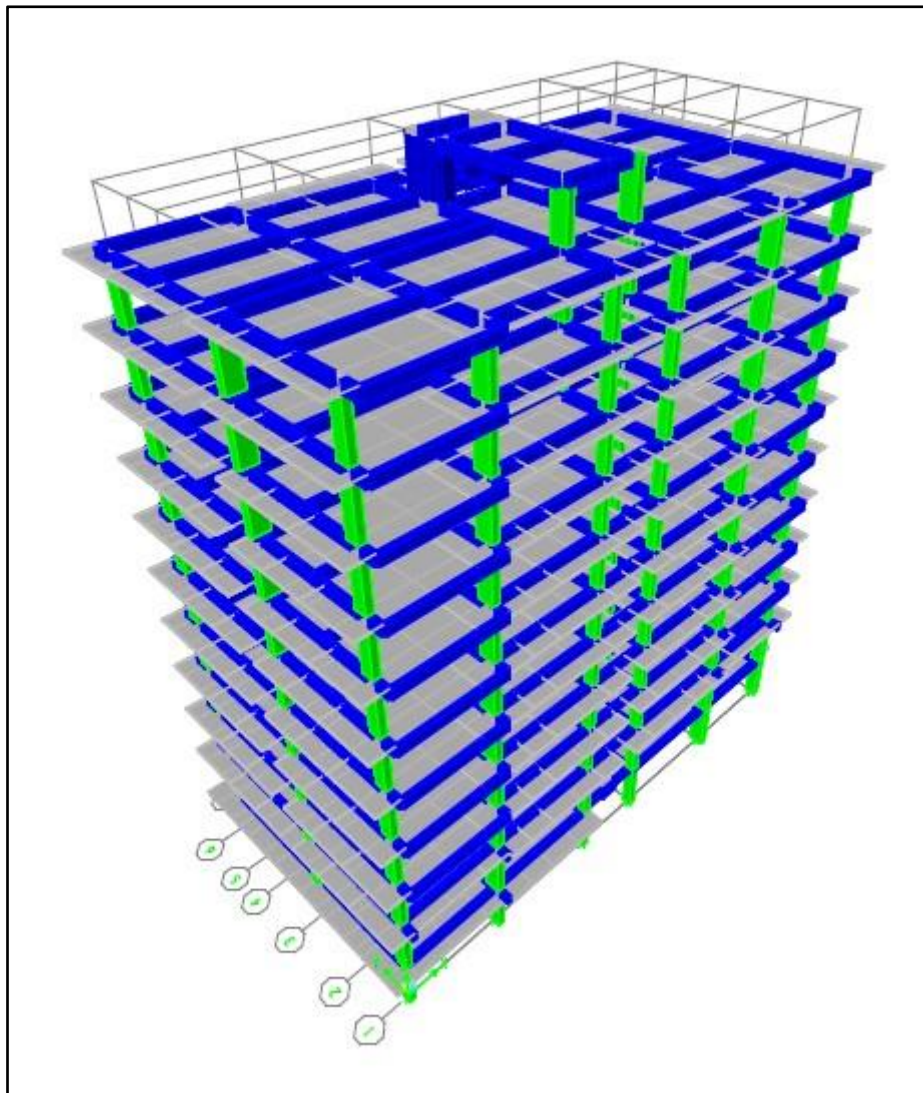


Figure 4.4: 3D View of 10 Story (G+9) Residential Building

Plan view of the selected model is presented in Figure 4.5.

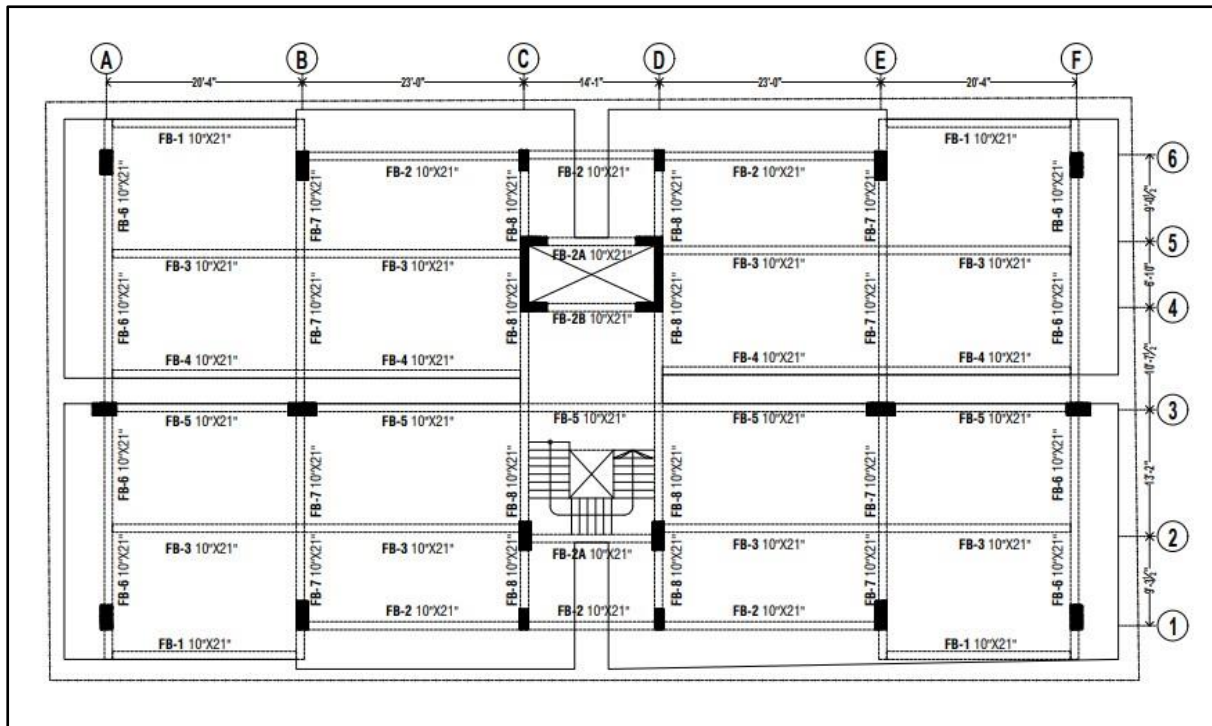


Figure 4.5: Plan View of 10 Story (G+9) Residential Building

Rebar Requirements of ground floor of this building have been calculated. There is a significant reduction in rebar consumption when higher grade steel is used. A mat foundation has been designed for this building using “SAFE” software. Comparison of rebar quantity for different grades of steel is shown in Table 4.6.

Table 4.6: Steel consumption comparison in mat foundation for different grades of steel

Rebar Grade, MPa	Rebar Requirement (in ² /ft)	Length (ft)	Rebar Requirement (in ³ /ft)	Savings of Steel Consumption
420	3.247	60	2337.8	0%
500	2.687	60	1934.6	17.22% w.r.t B420DWR
600	2.435	60	1753.2	25.0% w.r.t B420DWR 9.4% w.r.t B500CWR

B600 C-R will be cost effective for use in mat foundation. Total required beam rebar quantity of ground floor of this modeled residential building has been calculated as shown in Table 4.7.

Table 4.7: Ground floor Steel consumption comparison in beam for different grades of steel

Rebar Grade, MPa	Story	Rebar Requirement (m ³)	Rebar Requirement (kg)	Savings of Steel Consumption
420	Ground Floor	0.2249	1765.47	0%
500	Ground Floor	0.1896	1488.36	15.7% w.r.t B420DWR
600	Ground Floor	0.1575	1236.38	29.9% w.r.t B420DWR 16.9% w.r.t B500CWR

Total required column rebar quantity of ground floor of this modeled residential building has been calculated as shown in Table 4.8.

Table 4.8: Ground floor steel consumption comparison in column for different grades of steel

Rebar Grade, MPa	Story	Rebar Requirement (m ³)	Rebar Requirement (kg)	Savings of Steel Consumption
420	Ground Floor	0.447	3509	0%
500	Ground Floor	0.395	3101	11.6% w.r.t B420DWR
600	Ground Floor	0.383	3006	14.33% w.r.t B420DWR 3.1% w.r.t B500CWR

CHAPTER 5

CONCLUSIONS AND RECOMMENDATIONS

5.1 Introduction

The purpose of this study is to assess the performance of different structural members reinforced with different grades of rebar. Total twenty-seven specimens were tested. Nine beams were tested under two-point flexure test; nine columns were tested under compressive load and cyclic loading was applied for test on nine beam-column joint specimens. In addition to the experiments, design comparisons were made for beams, columns and two-way slabs designed with different grades of steel. A 10-storied reinforced concrete intermediate moment frame residential building was designed using different grades of steel. The reinforcement requirement at the ground floor and mat foundation of the building was compared. The findings of this research are presented in this chapter.

5.2 Conclusions from the Experiments

Major findings of the experiment are presented below:

- i. Moment capacity of beam increased 10.9% to 15.5% when reinforced with B600C-R in place of B420DWR and 2.5% to 4.7% when compared to B500CWR. For each class of concrete moment capacity of B600C-R was higher than B420DWR and B500CWR.
- ii. Load capacity of column, although being a compression member, increased about 7.3% to 18.1% when reinforced with B600C-R instead of B420DWR and about 2.1% to 9.6% when B600C-R is provided in lieu of B500CWR.
- iii. Grade of steel can also influence the lateral load carrying capacity of joints. Higher grade steel can sustain more number of cycles in push-pull cyclic test. Lateral load capacity also increased approximately 16.4% to 32.8% for B600C-R when compared to B420DWR and up to 14.2% when compared to B500CWR.

5.3 Conclusions from the Design Comparisons

Major findings from the design comparisons are presented below:

- i. In case of beam design, B600C-R reduces steel consumption up to 30% when compared to B420DWR and up to 16% when compared to B500CWR.

- ii. For columns designed with B600C-R, about 30% steel consumption is reduced when compared to B420DWR and about 16% is reduced when compared to B500CWR.
- iii. For slabs 31% reduction in steel is found when B600 C-R is compared to B420 DWR. This percentage reduces to 16% when B600 C-R is compared to B500CWR.

5.4 Conclusions from the Design of the 10-Storied Building

Major findings from the design comparisons are presented below:

- i. 25% saving is achieved in the design of mat foundation of the 10-storied building when B600C-R is used instead of B420DWR and 9.4% saving is possible compared to B500CWR.
- ii. For ground floor beams, B600C-R can save 29.9% and 16.9% steel as compared to B420DWR and B500CWR respectively.
- iii. Design of ground floor columns can be economized by 14.3% and 3.1%, respectively for B600C-R in comparison to B420DWR and B500CWR.

5.5 General Comments

Finally, in general, following comments can be made about using B600C-R.

- i. Use of B600C-R can substantially save steel consumption and reduce the cost of construction.
- ii. For similar loading condition, B600C-R offers congestion free sections contributing to better concreting.
- iii. Since lower diameter bars are required for B600C-R, less amount of development length and splice length are required.
- iv. Reduced requirement of steel implies reduced fabrication time and cost resulting in faster construction.
- v. Transport cost can also be curtailed due to less requirement of steel.
- vi. Energy demand for production steel will also decrease. Less amount of steel also implies less amount of exhaust gas and dust emissions during manufacturing process. All these factors will have positive impact on the environment and ensure sustainability.

5.6 Recommendations for Future Studies

A preliminary investigation of using higher grade steel in structural members has been performed in this study. Specimens have been prepared by using different grades of steel (B420 DWR, B500CWR, B600C-R) with different concrete classes to compare the results. Some areas where this research can be extended are presented below:

- i. Specimen reinforced with B600C-R can be cast with more high strength concrete. Higher strength concrete can be prepared by using admixture.
- ii. To get more information about stress strain pattern, strain gauges can be used.
- iii. Dynamic actuators and LVDTs can be used instead of manually operated push-pull jack and deflection dial gauges.
- iv. Finite element analysis can be adopted.

REFERENCES

- ACI 318-19 (2019). *Building Code Requirements for Structural Concrete*. American Concrete Institute.
- ASTM 615-20 (2020). *Standard Specification for Deformed and Plain Carbon-Steel Bars for Concrete Reinforcement*, American Society for Testing and Materials.
- ASTM 706-16 (2016). *Standard Specification for Deformed and Plain Low-Alloy Steel Bars for Concrete Reinforcement*, American Society for Testing and Materials
- BDS ISO 6935-2 (2021). Bangladesh Standards and Testing Institution, Bangladesh, International Organization for Standardization.
- BNBC (2020), Housing and Building Research Institute, Bangladesh, Bangladesh National Building Code.
- Cho, S., and Lee, J. (2019). Comparison of High Strength Re-Bar Usage by Type of Building Structure in Korea, *International Journal of Civil Engineering and Technology*, Volume 10, Issue 03, pp. 2936-2953.
- Cho, S., and Na, S. (2017). The Quantity Variations of the High-Strength Reinforcing Bars on the Underground Parking in a Rigid-Frame Building, *International Journal of Applied Engineering Research*, Volume 12, pp.1488-1499.
- KCI (2012), *Structural Concrete Design Code and Commentary*, Korea Concrete Institute.
- Kibria, B. M. G., (2014). Experimental investigation on behavior of reinforced concrete (RC) interior beam column joints retrofitted with fiber reinforced polymers (FRP). *M.Sc. thesis*. Department of Civil Engineering, Bangladesh University of Engineering and Technology, Dhaka.
- Kibria, B. M. G., Ahmed, F., Ahsan, R., and Ansary, M. A. (2020). Experimental investigation on behavior of reinforced concrete interior beam column joints retrofitted with fiber reinforced polymers. *Asian Journal of Civil Engineering*, 21, 157–171.
- Nilson, A. H., Darwin, D., and Dolan, C. W. (2010). *Design of Concrete Structures*, 14th Edition, *McGraw-Hill Companies, Inc.*

Pampanin, S., Calvi, G. M., Moratti, M. (2002). Seismic Behavior of R.C. Beam-Column Joints Designed for Gravity Only. *London: 12th European Conference on Earthquake Engineering, Sep 2002*. 726. Elsevier Science Ltd.

Siddique, A.F.A. and Ahsan, R. (2021). Structural Behavior of Reinforced Concrete Beam Column Joints under Cyclic Loading. *M.Sc. thesis*. Department of Civil Engineering, Bangladesh University of Engineering and Technology, Dhaka.

Siddique, A. F. A., Hossain, T. R. (2020). Seismic Performance Evaluation of Bridge Piers Resting on Different Soil Classes. *IABSE-JSCE Joint Conference on Advances in Bridge Engineering-IV*, Dhaka, Bangladesh.

Yao, X., Zhang, Y., Guan, J., Li, L., Liu, H., Han, R. and Xi, J.(2020). Experimental Study and Reliability Analysis of Flexural Capacity of RC Beams Reinforced with 600 MPa Grade Steel. *Advances in Civil Engineering*, Volume 2020, Article ID 8899630.

Short Biography of Principal Investigator

Professor Dr. Raquib Ahsan

Dr. Raquib Ahsan is a professor of Civil Engineering at the Bangladesh University of Engineering and Technology (BUET). He belongs to the Structural Engineering Division. He obtained B.Sc. and M.Sc. Engg. degrees from BUET in the years 1995 and 1997, respectively. He completed doctoral studies at Tokyo University in the year 2000. His fields of interest are structural dynamics, earthquake engineering, structural optimization, soil-structure interaction, structural retrofitting, etc. He conducted a large number of sponsored research. He has published over 80 book chapters and journal and conference articles. He acted as the Coordinator of the Bangladesh National Building Code

(BNBC) Updating project. He served as the Team Leader for many consultancy projects. The National Plan for Disaster Management (NPDM) 2021-2025 was drafted under his guidance. He is a member of the American Society of Civil Engineers (ASCE), American Concrete Institute (ACI), International Society of Soil Mechanics and Geotechnical Engineering (ISSMGE), and Institution of Engineers, Bangladesh (IEB).



Short Biography of Research Associate

A.S.M. Sawlat Rakin

A.S.M. Sawlat Rakin, a graduate civil engineer from the Bangladesh University of Engineering and Technology. He completed HSC from Notre Dame College and SSC from Cumilla Zilla School. While studying various construction materials and structural elements, he always wanted to work on a real project. In this project, his responsibilities included the estimation of materials, preparation of structural elements, execution of experiments, and analysis of the acquired data. While working on this project, he realized that the four years of undergraduate studies are just a hint of this vast field. To develop himself as a civil engineer having both practical and theoretical vision and to contribute more and better as a researcher, he is now pursuing M.Sc. in Structural Engineering.

